

**UNIVERSITY OF NAPLES FEDERICO II**



**PH.D. PROGRAM IN**  
**CLINICAL AND EXPERIMENTAL MEDICINE**  
*CURRICULUM IN TRANSLATIONAL MEDICAL SCIENCES*

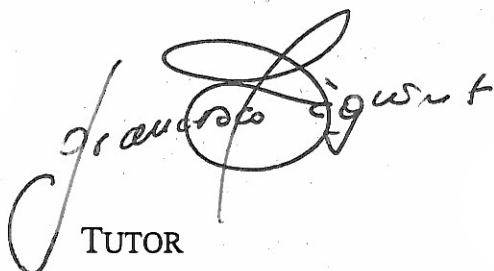
**XXX Cycle**  
*(Years 2014-2017)*

**Chairman: Prof. Gianni Marone**

**PH.D. THESIS**

**TITLE**

**Epigenetic modifications of the *ZNF423* gene control adipogenic commitment and are dysregulated in human hypertrophic obesity**

  
TUTOR

**Prof. Francesco Beguinot**



PH.D. STUDENT

**Dr. Michele Longo**

# **TABLE OF CONTENTS**

<b>LIST OF PUBLICATIONS</b>	<b>3</b>
<b>ABSTRACT</b>	<b>5</b>
<b>1. INTRODUCTION</b>	<b>6</b>
1.1 Obesity	6
1.2 Diabetes	9
1.3 The relationship between obesity and type 2 diabetes	10
1.4 Adipose tissue	12
1.4.1 Adipose tissue expansion: Subcutaneous vs. Visceral	13
1.4.2 White adipose tissue remodeling in obesity: Hypertrophy vs. Hyperplasia	14
1.4.3 Hypertrophic obesity is associated with restricted adipogenesis in subcutaneous adipose tissue	16
1.4.4 Hypertrophic obesity: inflammatory response and ectopic fat accumulation	18
1.5 Adipogenesis	20
1.6 Epigenetic and adipogenesis	22
<b>2. AIM OF STUDY</b>	<b>24</b>
<b>3. MATERIALS AND METHODS</b>	<b>25</b>
3.1 Materials	25
3.2 Cell culture and adipocyte differentiation	25
3.3 Participants	26

3.4 RNA isolation and quantitative real time RT-PCR	26
3.5 Micrococcal Nuclease (MNase) protection assay	27
3.6 DNA methylation assessment	28
3.7 <i>In-vitro</i> methylation and luciferase reporter assay	28
3.8 Site-direct mutagenesis and luciferase reporter assay	29
3.9 Statistical analysis	29
<b>4. RESULTS</b>	30
4.1 Promoter methylation reduces <i>Zfp423</i> expression in NIH-3T3 cells	30
4.2 Nucleosome occupancy of <i>Zfp423</i> promoter is increased in NIH-3T3 compared to 3T3-L1	32
4.3 5-Azacytidine enhances <i>Zfp423</i> expression and allows differentiation of non-adipogenic NIH-3T3 cells	34
4.4 BMP4 promotes <i>Zfp423</i> expression by inducing promoter demethylation	38
4.5 Preadipocyte <i>ZNF423</i> expression correlates with mature subcutaneous adipose cell size in humans	40
<b>5. DISCUSSION</b>	45
<b>6. REFERENCES</b>	49

## LIST OF PUBLICATIONS (Years 2014-2017)

1. **Longo M**, Raciti GA, Zatterale F, Parrillo L, Desiderio A, Spinelli R, Hammarstedt A, Hedjazifar S, Hoffmann JM, Nigro C, Mirra P, Fiory F, Formisano P, Miele C, Smith U and Beguinot F. **Epigenetic modifications of the *Zfp/ZNF423* gene control murine adipogenic commitment and are dysregulated in human hypertrophic obesity.**  
Diabetologia, 2017 Oct 24 [Epub ahead of print].
2. Ilaria Cimmino , Virginia Lorenzo , Francesca Fiory , Nunzianna Doti , Serena Ricci , Serena Cabaro , Antonietta Liotti , Luigi Vitagliano , **Michele Longo** , Claudia Miele , Pietro Formisano , Francesco Beguinot , Menotti Ruvo, Francesco Oriente. **A peptide antagonist of Prepl-p160 interaction improves ceramide-induced insulin resistance in skeletal muscle cells.**  
Oncotarget, 2017 May 03, 8(42):71845-71858.
3. Raciti GA, Spinelli R, Desiderio A, **Longo M**, Parrillo L, Nigro C, D'Esposito V, Mirra P, Fiory F, Pilone V, Forestieri P, Formisano P, Pastan I, Miele C, Beguinot P. **Specific CpG hyper-methylation leads to Ankrd26 gene down-regulation in white adipose tissue of a mouse model of diet-induced obesity.**  
Sci Rep. 2017 Mar 7;7:43526.
4. Nigro C, Leone A, Raciti GA, **Longo M**, Mirra P, Formisano P, Beguinot F, Miele C. **Methylglyoxal-Glyoxalase 1 Balance: The Root of Vascular Damage.**  
Int J Mol Sci. 2017 Jan 18;18(1).
5. Mirra P, Nigro C, Prevenzano I, Procopio T, Leone A, Raciti GA, Andreozzi F, **Longo M**, Fiory F, Beguinot F, Miele C. **The role of miR-190a in methylglyoxal-induced insulin resistance in endothelial cells.**  
Biochim Biophys Acta. 2017 Feb;1863(2):440-449.
6. Ariemma F, D'Esposito V, Liguoro D, Oriente F, Cabaro S, Liotti A, Cimmino I, **Longo M**, Beguinot F, Formisano P, Valentino R. **Low-Dose Bisphenol-A Impairs Adipogenesis and Generates Dysfunctional 3T3-L1 Adipocytes.**  
PLoS One. 2016 Mar 4;11(3):e0150762.
7. **Longo M**, Spinelli R, D'Esposito V, Zatterale F, Fiory F, Nigro C, Raciti GA, Miele C, Formisano P, Beguinot F, Di Jeso B. **Pathologic endoplasmic reticulum stress induced by glucotoxic insults inhibits adipocyte differentiation and induces an inflammatory phenotype.**  
Biochim Biophys Acta. 2016 Jun;1863(6 Pt A):1146-56
8. Ciccarelli M, Vastolo V, Albano L, Lecce M, Cabaro S, Liotti A, **Longo M**, Oriente F, Russo GL, Macchia PE, Formisano P, Beguinot F, Ungaro P. **Glucose-induced**

**expression of the homeotic transcription factor Prep1 is associated with histone post-translational modifications in skeletal muscle.**

Diabetologia. 2016 Jan;59(1):176-86.

9. Parrillo L, Costa V, Raciti GA, **Longo M**, Spinelli R, Esposito R, Nigro C, Vastolo V, Desiderio A, Zatterale F, Ciccodicola A, Formisano P, Miele C, Beguinot F. **Hoxa5 undergoes dynamic DNA methylation and transcriptional repression in the adipose tissue of mice exposed to high-fat diet.**

Int J Obes (Lond). 2016 Jun;40(6):929-37.

10. Raciti GA, **Longo M**, Parrillo L, Ciccarelli M, Mirra P, Ungaro P, Formisano P, Miele C, Béguinot F. **Understanding type 2 diabetes: from genetics to epigenetics.**

Acta Diabetol. 2015 Oct;52(5):821-7.

11. Borriello F, **Longo M**, Spinelli R, Pecoraro A, Granata F, Staiano RI, Loffredo S, Spadaro G, Beguinot F, Schroeder J, Marone G. **IL-3 synergizes with basophil-derived IL-4 and IL-13 to promote the alternative activation of human monocytes.**

Eur J Immunol. 2015 Jul;45(7):2042-51.

## ABSTRACT

Subcutaneous adipocyte hypertrophy is typically associated with insulin resistance and increased risk of type 2 diabetes and predicts its future development independent of obesity. In humans, subcutaneous adipose tissue hypertrophy is a consequence of impaired adipocyte precursor cell recruitment into the adipogenic pathway rather than lack of precursor cells but the molecular events responsible for the restricted adipogenesis remain unclear. The zinc-finger transcription factor (Zfp) 423 has been identified as a major determinant of preadipocyte commitment and maintained white adipose cell function. Although its levels do not change during adipogenesis, ectopic expression of *Zfp423* in non-adipogenic cells is sufficient to activate peroxisome proliferator-activated receptor gamma (*Pparγ*) expression and to increase the adipogenic potential of these cells.

In the present work, we have investigated whether *Zfp423* is epigenetically regulated and whether these events are involved in the restricted adipogenesis in humans with expanded subcutaneous adipose tissue.

We report here that, comparison of uncommitted (NIH-3T3) and committed (3T3-L1) adipose precursor cells revealed that *Zfp423* expression increased in parallel with the ability of the cells to differentiate into mature adipocytes owing to both decreased promoter DNA methylation and nucleosome occupancy in the 3T3-L1 compared with NIH-3T3 cells. Interestingly, non-adipogenic epigenetic profiles can be reverted in NIH-3T3 cells as 5-azacytidine treatment increased *Zfp423* mRNA levels, reduced DNA methylation at a specific CpG site, decreased nucleosome occupancy and induced adipocyte differentiation. These epigenetic modifications can also be initiated in response to changes in the pre-adipose cell microenvironment, in which bone morphogenetic protein 4 (Bmp4) plays a key role. We finally showed that, expression of the *ZNF423* human ortholog in adipocyte precursor cells from subcutaneous adipose tissue inversely correlated to cell size of the autologous mature adipocytes. Promoter methylation at the *ZNF423* regulatory region also reflected inappropriate subcutaneous adipose cell hypertrophy. As in NIH-3T3 cells, the normal *ZNF423* epigenetic profile was rescued by 5-azacytidine exposure.

Thus, our results show that epigenetic events regulate the ability of precursor cells to commit and differentiate into mature adipocytes by modulating *ZNF423* expression, and indicate that dysregulation of these mechanisms accompanies subcutaneous adipose tissue hypertrophy in humans.

# 1. INTRODUCTION

## 1.1 Obesity

Obesity is a serious global health challenge, especially in developed and developing countries, representing a major health problem that has a priority in public health policies (Pardo et al. 2012). The prevalence of obesity has been dramatically rising in the last 30-50 years (Al-Goblan et al. 2014); indeed, if this trend continue, an estimated 38% of the world's adult population will be overweight and another 20% will be obese in 2030 (Kelly et al. 2008). More than 1 in 3 adults is obese in the United States, Mexico, and New Zealand, and more than one in four in Australia, Canada, and Chile. (Fig. 1).

A positive note is that the overweight rate is almost stabilized in Italy in the past ten years and obesity rates are among the lowest in the Organization for Economic Cooperation and Development (OECD) countries. Indeed, only 1 in 10 adults is obese in Italy, significantly less than the OECD average of 1 in 6 (OECD, update 2014). However, childhood obesity rate is notoriously one of the highest (36% for boys and 34% for girls) (OECD, update 2014, Italy).

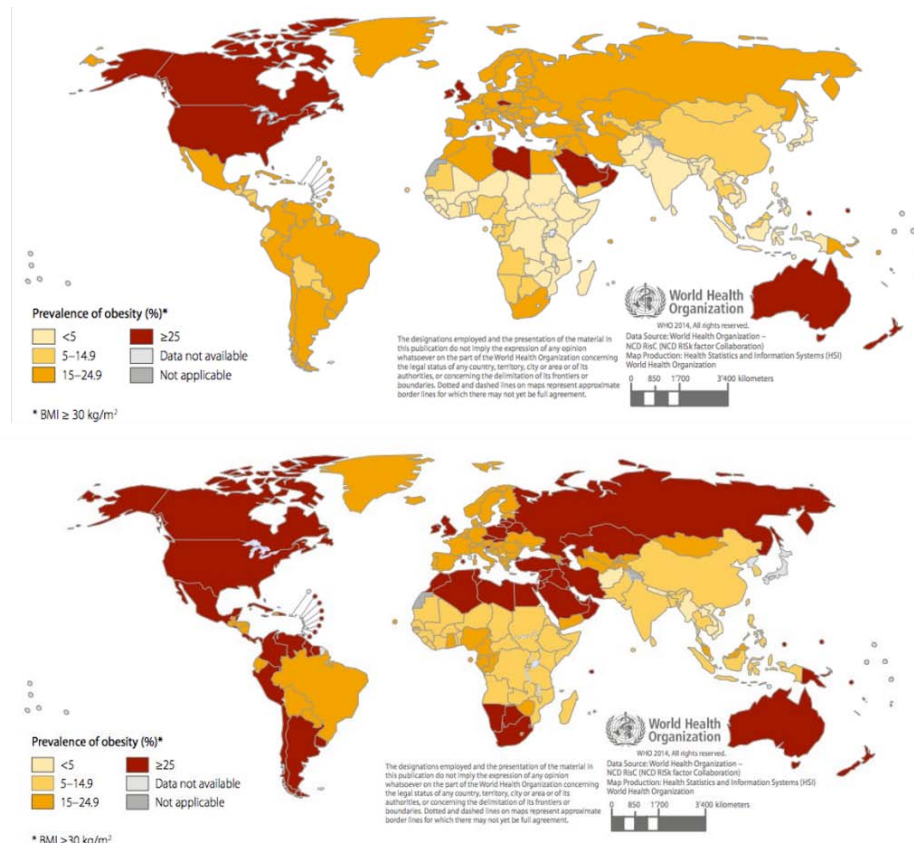


**Figure 1. Prevalence of obesity in adulthood.** The maps indicate the adult prevalence of obesity respectively in males and females (World Health Organization 2014).

Obesity is characterized by an increased body weight due to an altered imbalance between energy intake and energy expenditure and is defined as a condition characterized by an excess of fat accumulation in adipose tissue, to an extent that impairs both physical and psychosocial health (Kopelman 2000).

In clinical practice, the most simply and widely used method for classifying obesity is the body mass index (BMI= body weight in kg/ height in m<sup>2</sup>), which ranges from underweight (<18.5 kg/m<sup>2</sup>) to severe or morbid obesity (≥40 kg/m<sup>2</sup>), (Table 1), (World Health Organization 2014).

Category	BMI range (kg/m <sup>2</sup> )
Underweight	< 18.5
Normal weight	18.5 - 24.9
Overweight	25.0 - 29.9
Obese	30.0 - 39.9
Morbidly obese	≥ 40.0

**Table 1. Classification of adult underweight, overweight and obesity according to BMI.** According to WHO, overweight is defined as a BMI equal to or more than 25 whereas obesity as a BMI equal to or more than 30 (World Health Organization 2014).

A significant increase in the mortality risk starts as the BMI increases over 25 (Speakman et al. 2004). This is because there is a strong correlation between body fat and the incidence of several chronic diseases, such as cancer, coronary heart disease and diabetes mellitus. The effects of obesity on health outcome appear to be reversible if the person in question loses weight; indeed a modest weight loss of 5%-10% of body weight has been shown to significantly improve cardiometabolic risk factors (Brown et al. 2015) (Fig. 2).



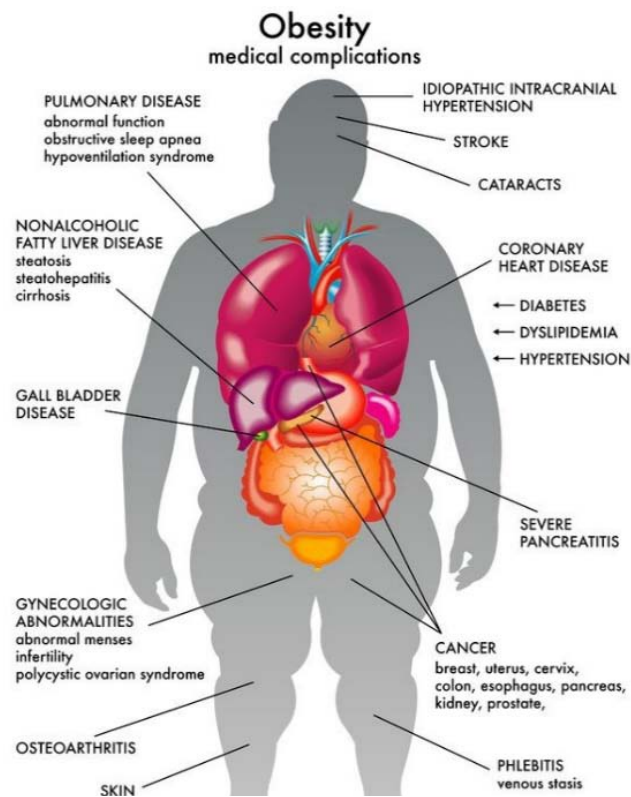


**Figure 2. Representation of the most important comorbidities associated with obesity.** Obesity has a multitude of adverse metabolic health consequences such as diabetes mellitus, hypertension, dyslipidemia, and metabolic syndrome (Kopelman 2000).

Obesity is a multifactorial disease arising from a complex interaction between genetic, developmental, behavioural, and environmental influences (Chung et al. 2008, Speakman et al. 2004). Evidence for genetic contributions to human obesity is provided by familial clustering of increased adiposity, including a three to seven fold increased relative risk among siblings (Chung et al. 2008, Allison et al. 1996). Genetic factors are currently estimated to account for 40–70% of the variance in human adiposity (Chung et al. 2008, Allison et al. 1996). However, the dramatic increase in obesity prevalence observed in the last decade seems attributable mainly to environmental changes promoting the intake of energy-dense foods and/or reduced physical activity (Dalle Grave et al. 2013). To reverse the obesity epidemic, community efforts should focus on creating a healthy environment favouring the adoption of healthy behaviours through an incisive public health intervention. However, it is doubtful that the obesity-promoting environment will change in the near future. For this reason, it is essential to develop more efficacious strategies to help individuals to adopt a healthy lifestyle in a “toxic” environment favouring the development of a positive energy balance (Chung et al. 2008).

## 1.2 Diabetes

Diabetes mellitus is a chronic metabolic syndrome characterized by elevated blood glucose levels (hyperglycaemia) caused by defects in insulin secretion, insulin action or both (American Diabetes Association 2010). According to the classification recommended by the American Diabetes Association, there are three main form of diabetes: type 1 diabetes (T1D), type 2 diabetes (T2D), and gestational diabetes mellitus (American Diabetes Association 2010).

T1D, once known as insulin-dependent diabetes, is a chronic condition characterized by an absolute deficiency of insulin, resulting from an autoimmune mediated destruction of  $\beta$  cells. Patients with T1D require a daily injection of insulin for survival.

T2D is the most common form of diabetes mellitus and is characterized by decreased insulin sensitivity, as a result of insulin resistance in peripheral tissue, insulin secretory defect of the beta cell and excessive hepatic glucose production (Harrison 2009). The most recent T2D treatment guidelines indicate to begin with an individualized approach, consisting initially of dietary control and lifestyle modifications, followed by oral hypoglycaemic agents and, if the control of glucose homeostasis is not achieved, insulin therapy is required (American Diabetes Association 2015).

The chronic hyperglycaemia associated with diabetes leads to long term macro- and microvascular complications. Microvascular complications result from damage to small blood vessels and include damage to the nervous system (neuropathy), renal system (nephropathy) and eye (retinopathy). The major macrovascular complications include accelerated cardiovascular disease resulting in higher risk of coronary artery disease, peripheral arterial disease, myocardial infarction, stroke, and limb amputation (World Health Organization 2010).

Diabetes may be diagnosed based on either one of the four plasma glucose criteria: 1) fasting plasma glucose (FPG)  $>126$  mg/dL, 2) 2 h plasma glucose during a 75-g oral glucose tolerance test (OGTT)  $>200$  mg/dL, 3) random plasma glucose  $>200$  mg/dL with classic signs and symptoms of hyperglycaemia, or 4) Glycated haemoglobin (HbA1c) level  $>6.5\%$  (American Diabetes Association 2015). T2D mellitus is a common and increasingly prevalent disease, representing one of the major and serious public health burden (Tabish 2007). The International Diabetes Federation estimates that there are approximately 387 million people in the world affected with diabetes and globally, it is expected to afflict around 592 million people by 2035 (International Diabetes Federation Atlas 2013) (Fig. 3). The American Diabetes Association has released a range of recommendations called Standards of Medical Care in Diabetes to improve diabetes outcomes. The recommendations include cost-effective screening, diagnostic and therapeutic strategies to prevent, delay, or effectively manage T2D and its complications (American Diabetes Association 2014).

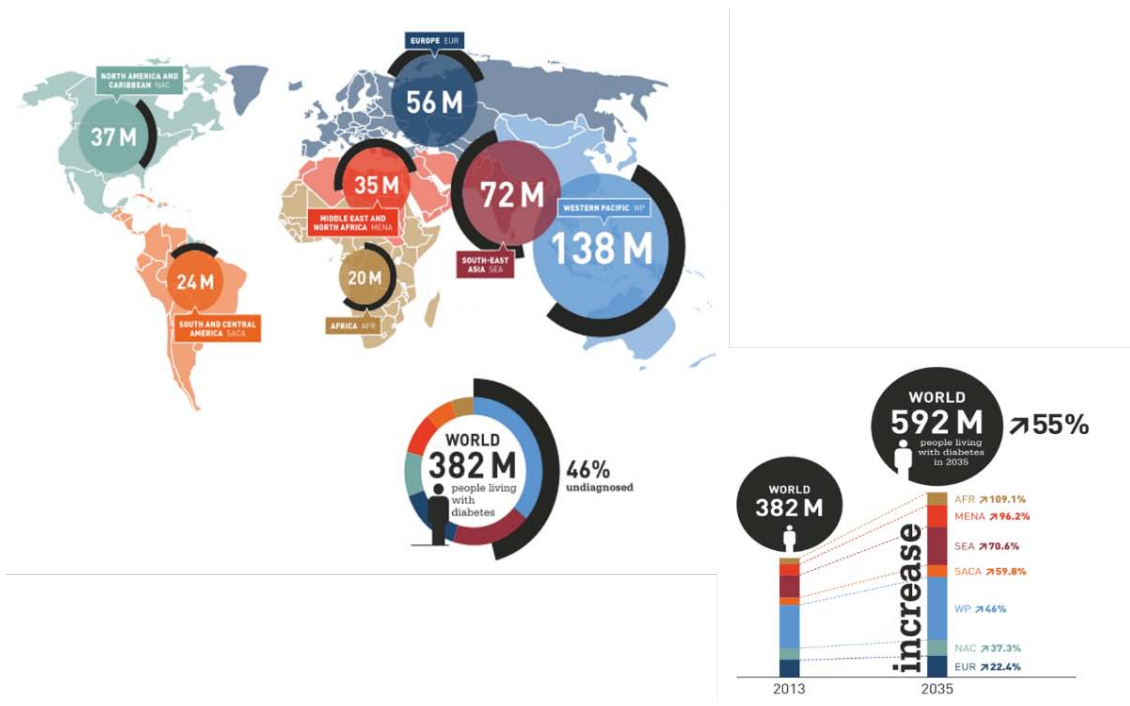


**Figure 3. World Prevalence of diabetes.** *The International Diabetes Federation Atlas (IDF Atlas 2013) figure provides a worrying indication of the future impact of diabetes on the global development.*

### 1.3 The relationship between obesity and Type 2 diabetes

Obesity and T2D are the major public health problems throughout the world and are associated with significant co-morbidities and enormous economic costs. The prevalence of overweight and obesity is increasing rapidly worldwide, especially in developing countries. There is a strong association between obesity and T2D. Meta-analysis of association studies showed a higher relative risk for T2D with BMI above 23 as well as a higher waist circumference in both men and women (Fig. 4) (Guh et al. 2009, Yaturu et al. 2011, Ni Mhurchu et al. 2006). Particularly, the prevalence of diabetes increase from 2% in individuals with a BMI between 25 and 29.9 kg/m<sup>2</sup>, to 8% in those with a BMI of 30 to 34.9 kg/m<sup>2</sup>, and finally to 13% in those with a BMI greater than 35 kg/m<sup>2</sup> (Harris et al. 1998).

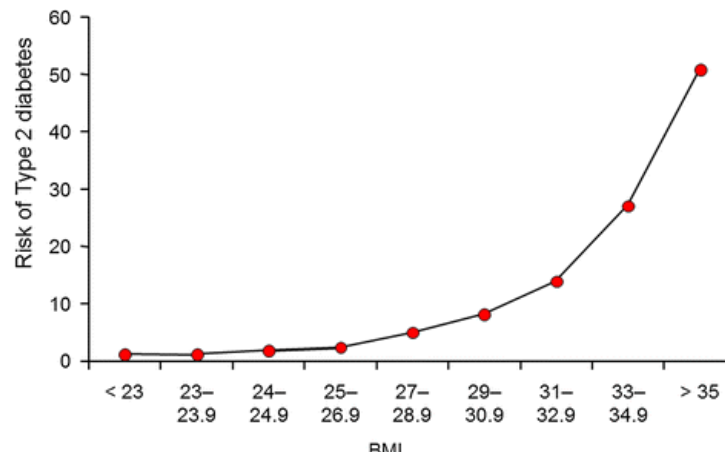


**Figure 4. BMI and type 2 diabetes risk.** The relationship between BMI and risk to develop type 2 diabetes (Sattar et al. 2014).

Prospective studies in overweight non-diabetic adults reveal a 49% increase in the diabetes incidence in 10 years for every 1 kg/year increase in body weight and each kg of weight lost annually over 10 years was associated with a 33% lower risk of diabetes. Furthermore, studies in Pima Indians showed that weight gain was strongly related to diabetes incidence only in those who were not initially overweight (Aucott 2008, Resnick et al. 2000).

Glycaemic control is guaranteed by an accurate balance between insulin secretion by the pancreatic  $\beta$ -cells and insulin sensitivity of the peripheral tissues and insulin resistance is a key feature of the metabolic syndrome progression to T2D. Decreased insulin sensitivity and insufficient insulin production are the two key element in T2D pathogenesis (Yaturu et al. 2011) and insulin resistance represents the major link between obesity and T2D. In the natural history of diabetes, obesity and insulin resistance precede the alterations in glucose homeostasis. Insulin resistance in both of these conditions is manifested by decreased insulin-stimulated glucose transport in adipocytes and skeletal muscle and by impaired suppression of hepatic glucose production (Reaven et al. 1995).

Nevertheless, not all subjects with T2D are obese and many obese individuals do not show diabetes or the other metabolic complications typical of obesity (10-30%) (Kloting et al. 2010). Thus, BMI *per se* is not a sufficiently sensitive marker of individual risk for obesity-related metabolic complications. Growing evidence suggest an important role for the regional fat distribution in the development of adverse metabolic complications (Karpe et al. 2015; Lee et al. 2013). Recently, the subcutaneous adipose tissue is generating increasing interest, indeed, its impaired expandability and the consequent inappropriate expansion of adipose cells are associated with increased local and systemic inflammation, insulin resistance, and ectopic fat accumulation, considered to be the main determinant of the obesity-related metabolic complications (Gustafson et al. 2015; Kloting et al. 2014; Sun et al. 2011).

## 1.4 Adipose tissue

Until the late 1940s, adipose tissue was considered an energy storage connective tissue, without any implication in the regulation of energy balance (Rosen et al. 2006).

Over the years, this began to change with the realization that adipose tissue plays a major role in nutrient homeostasis, serving as the site for calorie storage, as the source of circulating free fatty acids during fasting and as an endocrine organ producing adipose-derived serum factors (Rosen et al. 2014). Moreover, the growing incidence of obesity and associated metabolic comorbidities has raised the urgency in understanding all aspects of adipose tissue biology.

Depending on the nature of the adipocytes, the mammalian adipose tissue is divided into two functionally distinct forms of fat: white and brown (Fig. 5), (Ronti et al. 2006; Rosen et al. 2006).

The white adipocyte is the primary site of energy storage and is characterized by the presence of a large unilocular lipid droplet acting as a safe storage compartment for triglycerides (Hepler et al. 2017).

Furthermore, white adipose tissue (WAT) also has mechanical properties, serving to protect organs from mechanical damage and secretes hormones and cytokines, termed “adipokines,” that regulate glucose homeostasis, lipid metabolism and inflammation (Deng et al. 2010).

Mammals also contain “brown” adipocytes and their main function is to convert chemical energy into heat. Brown adipocytes are characterized by their multilocular lipid droplet appearance and high mitochondrial content (Hepler et al. 2017, Cannon et al 2004). The thermogenic program of brown adipocytes is mediated by the expression of uncoupling protein 1 (UCP1) a brown adipose tissue-specific protein located within the mitochondria (Klingenberg et al. 1999).

In addition to brown and white fat depots, prolonged cold exposure or adrenergic signaling can induce the formation of subsets of UCP-1 positive cells with a brown-like morphology within white fat depots. These inducible cells called “beige” or “brite” adipocytes have an overlapping but distinct gene expression pattern compared to classic brown adipocytes (Wu et al. 2012). The ability to induce “browning” of WAT in rodents is protective against obesity and can reverse insulin resistance in metabolic syndrome (Hepler et al. 2017, Rajakumari et al. 2013). Some of these effects may be mediated by the thermogenic capacity of these cells; others may be mediated by an endocrine function.

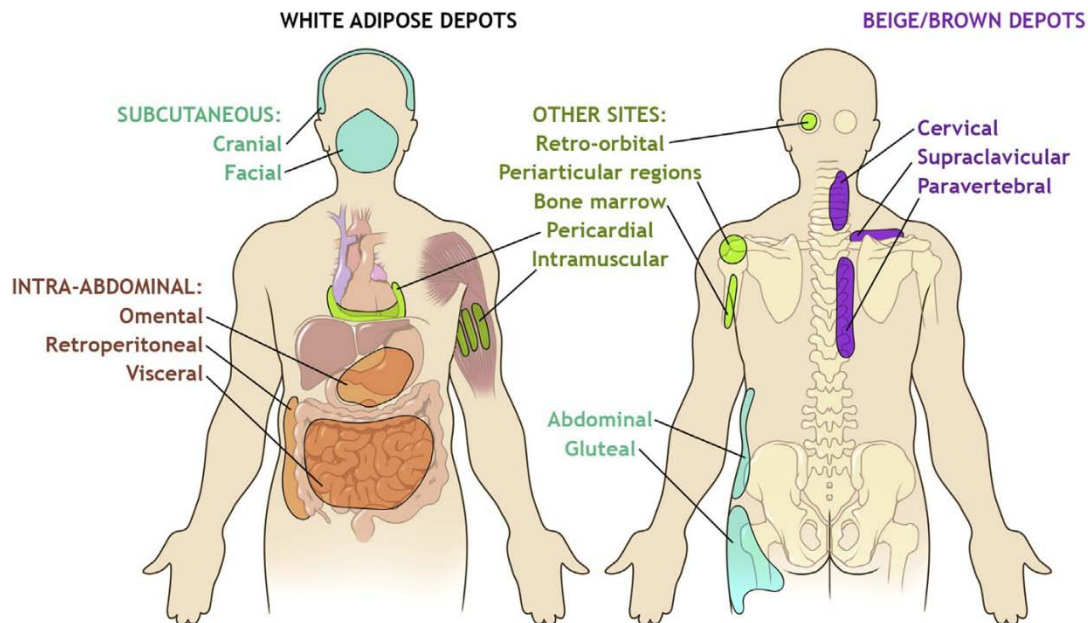


**Figure 5.** Distribution of White and Brown/Beige Adipose Tissue in Adults. WAT is organized into distinct depots, classified by location as subcutaneous or intra-abdominal.

The major subcutaneous WAT includes the abdominal, gluteal, and femoral depots. Brown adipose tissue depots are located in the cervical, supraclavicular, and paravertebral regions in adults (Hepler et al. 2017).

#### 1.4.1 Adipose tissue expansion: Subcutaneous vs. Visceral

WAT has an incredible ability to expand its dimension as the request for energy storage increases. Expansion of WAT is a physiologically response to caloric excess; however, obesity is associated with increased risk for diabetes and insulin resistance. Although weight excess is the primary risk factor for T2D obesity is not a homogeneous condition. Indeed, approximately 10-30% of obese individuals do not show the associated metabolic complications (Appleton et al. 2013; Denis et al. 2013). There is growing interest in better identifying clinical parameters correlating with obesity and its associated diseases. Notably body fat distribution is one of best predictors of metabolic health in obesity (Karpe et al. 2015; Lee et al. 2013). Subcutaneous adipose tissue (SAT) stores more than 80% of total body fat and is located beneath the skin; while visceral fat surrounds internal organs, and comprises less than 10% of the total fat mass (Hepler et al. 2017).

WAT is now considered as the center of the disorder and its associated comorbidities (Greenberg et al. 2006). Obese people, who preferentially accumulate excess adiposity in the visceral region, are at higher risk than those who accumulate adipose tissue in the subcutaneous compartment.

There is also a dimorphism in the anatomical distribution of fat tissue (Karastergiou et al. 2012; Hepler et al. 2017). In women, adipose accumulation occurs preferentially in the subcutaneous regions; while in men, visceral WAT expansion is more evident and role of sex hormones is now well recognized (Davis et al. 2013; Palmer et al. 2015). One possible reason for the detrimental effects of visceral adipose accumulation is the location of the depot itself. Lipids and metabolites can be released into the portal circulation and affect liver function (Rytka et al. 2011). However, the observation that anatomically distinct adipocytes follow two different development processes, raises the possibility that they are also functionally (and intrinsically) distinct. Adipose depot transplantation experiments in mice indicate that factors intrinsic to these depots determine their effect on glucose homeostasis (Tran et al., 2008). Indeed, several studies demonstrate that adipocytes, from different fat depots, are functionally unique, differing in their ability to undergo lipolysis, lipogenesis, and activate thermogenic programs (Lee et al. 2013; Macotela et al. 2012; Wu et al. 2012). Thus, an emerging hypothesis is that anatomically distinct WAT depots likely represent distinct “mini-organs.” A better understanding of how these distinct depots arise and expand during development may lead to therapeutic strategies to alter body fat distribution.

#### **1.4.2 White adipose tissue remodeling in obesity: Hypertrophy vs. Hyperplasia**

In response to nutrient excess WAT expands through the enlargement of existing adipocytes (adipocyte hypertrophy) or through the formation of new adipocytes (adipocyte hyperplasia) (Hirsch et al. 1969). As shown by several studies, the balance between these two mechanisms depends on the location of the fat pad. However, in humans, the mechanisms of adipose tissue expansion during obesity are not fully delineated. Analysis of adipocyte size and number in adults before and after weight gain suggest that females expand lower-body subcutaneous depots through adipocyte hyperplasia while males expand these same depots through hypertrophy (Tchoukalova et al., 2010).

Furthermore, it has been reported that new adipocytes are generated constantly to replace lost adipocytes (Spalding et al. 2008), and estimated that the adipocyte half-life is in the order of 8.3 years (Sun et al. 2011). Moreover, evidence suggest that the number of adipocytes is already fixed in childhood and a significant weight loss is associated only with reduction of adipocyte size and not of their number (Sun et al. 2011; Spalding et al. 2008).

Nevertheless, the patterns of fat deposition and expansion vary between people and this variance determines the differences found in metabolic disease risk seen among individuals with a similar BMI.

Several analyses of WAT from obese individuals reveal that adipocyte size and number correlate well with the risk of metabolic syndrome, independent of BMI (Gustafson et al.



2015; Hepler et al. 2017; Kloting et al. 2010). WAT from patients with metabolic syndrome is characterized by hypertrophic adipocytes, hypoxia, fibrosis, and inflammation (Gustafson et al. 2015; Kloting et al. 2014; Sun et al. 2011). The exact sequence of events is still unclear; however, (Fig. 6) the inability of SAT to enlarge through hyperplasia leads to burdened and hypoxic adipocytes and in this scenario, adipose cell death can occur, leading to the recruitment of immune cells and initiation of inflammation. Indeed, the ability of the WAT to act as a safe storage depot is impaired, inducing other peripheral tissues to compensate by accumulating inappropriately lipids, including the liver and the skeletal muscle, thus triggering local and systemic insulin resistance (Chaurasia et al. 2015; Perry et al. 2014). On the contrary, SAT from metabolically healthy individuals is characterized by numerous and relatively smaller adipocytes (Corvera et al. 2014; Kloting et al. 2010).

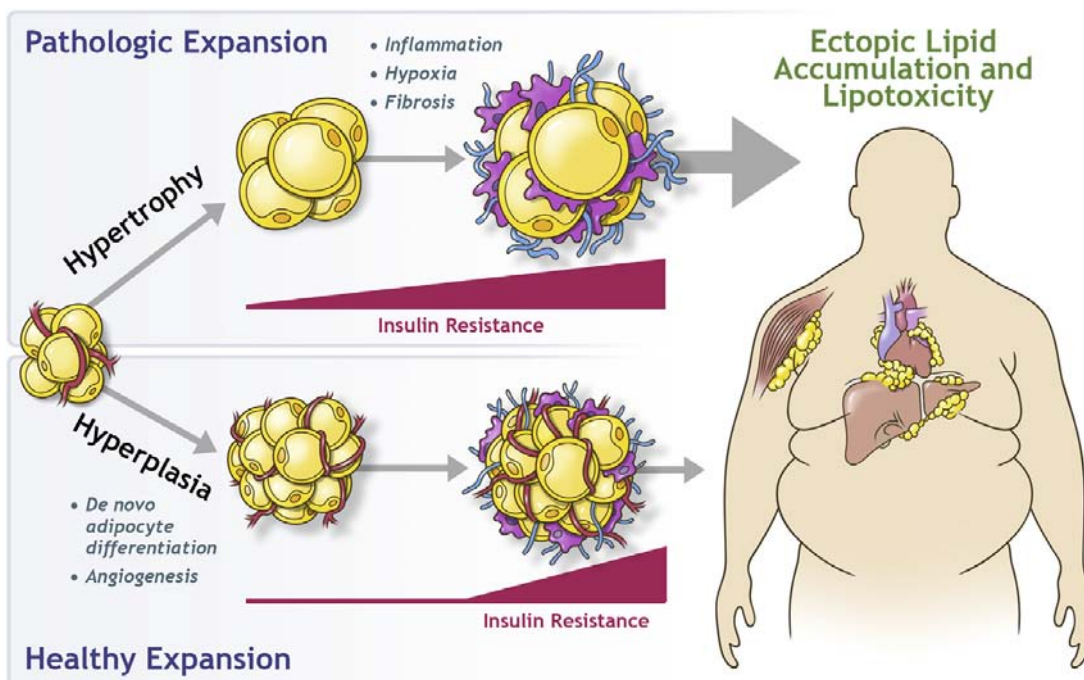


**Figure 6. White Adipose Tissue Expansion in Obesity.** Expansion of white adipose tissue in response to caloric excess occurs through the enlargement of existing adipocytes (hypertrophy) and/or through an increase in adipocyte number (hyperplasia). Pathologic expansion through hypertrophy of adipocytes is associated with inflammation, hypoxia, and fibrosis, with early onset of insulin resistance. Adipocyte dysfunction leads to the deleterious spillover of lipids into non-adipose organs, termed lipotoxicity. Healthy expansion through hyperplasia of adipose tissue occurs through the recruitment of preadipocytes and de novo adipocyte differentiation. This occurs alongside with angiogenesis and prevents or delays the onset of both insulin resistance and ectopic lipid accumulation (Hepler et al. 2017).



### 1.4.3 Hypertrophic obesity is associated with restricted adipogenesis in SAT

The limited expandability of the subcutaneous adipose tissue leads to an inappropriate adipose cell expansion (hypertrophic obesity) with local inflammation and insulin-resistant phenotype (Neeland et al. 2012, Weisberg et al. 2003).

Promoting adipose cell recruitment in the subcutaneous adipose tissue rather than merely inflating the cells, would be protective from the obesity-associated metabolic complications. Previous studies have shown that increased subcutaneous fat cell size in humans negatively correlates with insulin sensitivity independent from obesity (Smith et al. 2010), moreover it has been shown to be an independent risk factor of T2D in prospective studies (Lönn et al. 2010).

In a large study, Smith and colleagues analyzed adipogenic potential of preadipocytes isolated from the stromal-vascular fraction (SVF) cells from SAT (Gustafson et al. 2012) finding significant differences between donors in the number of cells that underwent adipogenesis under identical conditions. In fact, some individuals exhibit only 5–10% of cells undergoing differentiation while, in others, 80% of the cells became adipocytes (Gustafson et al. 2012). Interestingly, reduced differentiation was seen in individuals characterized by increased adipose cell size (hypertrophic SAT), whereas small adipocytes were associated with good adipogenesis (Fig. 7) suggesting a causal relationship. It is important to note that poor adipogenesis is not due to lack of precursor cells but rather to the inappropriate signaling of pathways promoting precursor cell commitment and differentiation (Talchai et al. 2012).

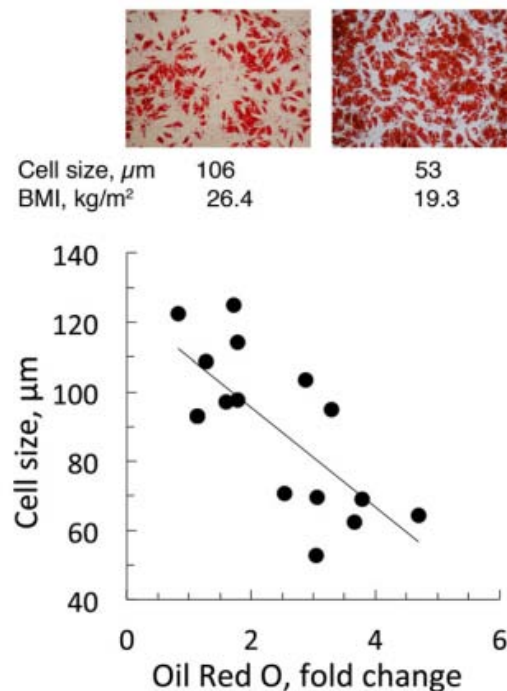


**Figure 7. Adipogenic potential of human preadipocytes from the subcutaneous adipose tissue is associated to the adipose cell size of the donors. SVF preadipocytes were differentiated for 21 days in vitro and then stained with Oil Red O to show the lipid droplets (top). The negative correlation between the amount of lipids accumulated during differentiation and the adipose cell size of the donors is shown (bottom) (Gustafson et al. 2012).**

Furthermore, Smith and colleagues (Hammarstedt et al. 2013; Gustafson et al. 2013) have also identified the WNT-inducible secreted protein 2 (WISP2) that is highly expressed in early adipogenic precursor cells. This protein inhibits adipogenesis by dual mechanisms. In the first, cytosolic WISP2 forms a complex with the zinc finger protein 423 (Zfp423) that is a transcriptional activator of  $PPAR\gamma$ . This complex is dissociated by bone morphogenetic protein 4 (BMP4), allowing *Zfp423* to enter into the nucleus and initiate *Ppar $\gamma$*  activation. However, WISP2 is also a secreted protein that directly can inhibit *Ppar $\gamma$*  activation although the mechanism is still unclear (Fig. 8), (Hammarstedt et al. 2013; Gustafson et al. 2013). Interestingly, they also found WISP2 expression increased in the SAT compared to VAT, moreover, WISP2 SAT expression is higher in individuals with hypertrophic adipose tissue and correlates with the ectopic fat accumulation (Gustafson et al. 2013). Thus, restricted adipogenesis in SAT is currently considered a novel susceptibility factor for T2D and this is also evident in non-obese individuals (Arner et al. 2011).

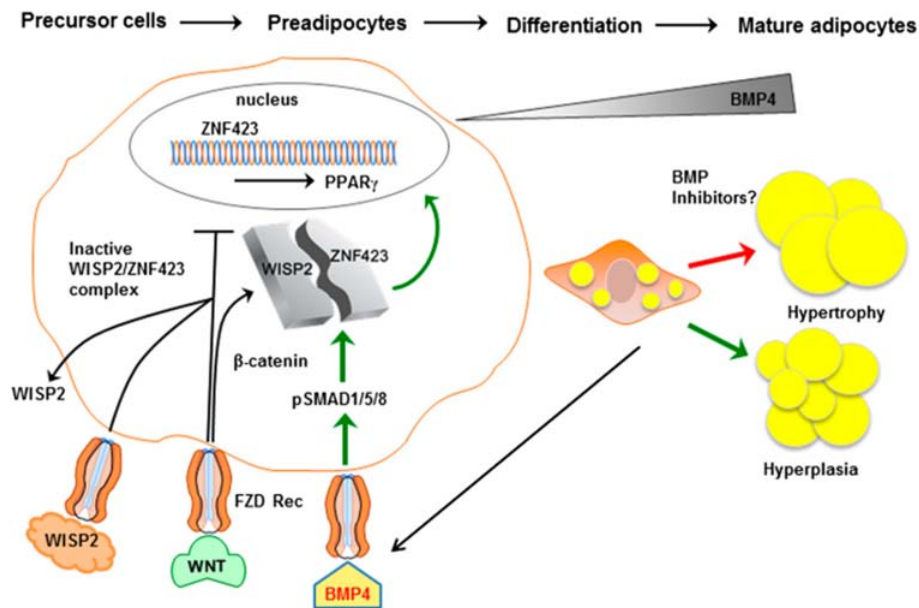


***Figure 8. Preadipocyte commitment.** Precursor cells are kept undifferentiated by WNT activation and WISP2. WISP2 prevents PPAR $\gamma$  activation by binding Zfp423 in the cytosol. BMP4 dissociates the complex, allowing Zfp423 to enter in the nucleus and initiate PPAR $\gamma$  activation (Hammarsted et al. 2013).*

#### **1.4.4 Hypertrophic obesity: inflammatory response and ectopic fat accumulation**

Adipocyte volume is also associated with increased inflammatory circulating factors, oxidative stress and an increased infiltration of macrophages within adipose tissue. In SAT, these alterations cause the shifting toward proinflammatory adipokines secretion pattern (Klötting et al. 2014; Blüher et al. 2013) and the onset of the chronic low-grade inflammation (Sell et al. 2012).

Adipocytes and macrophages can react to these stress stimuli by the activation of stress-sensing pathways, which may contribute to the deterioration of cellular functions and contribute to the metabolic comorbidities associated with obesity (Rudich et al. 2007; Bashan et al. 2007). In addition, macrophages may report to other organs the stress and inflammatory status of the adipose tissue, leading to secondary organ failure. In conclusion, hypertrophic obesity may start a sequence of pathogenic event that contributes to adipose tissue dysfunction and subsequent effects on other tissues (Blüher et al. 2013).

Many evidence suggest that both restricted adipogenesis and the impaired tissue vascularization capacity are responsible for the onset of metabolic diseases (Gealekman et al. 2011; Van Harmelen et al. 2004). The inability of SAT to expand proportionally to caloric excess represents an important link in the development of adipose tissue dysfunction and ectopic fat accumulation (Blüher et al. 2013; Van Harmelen et al. 2004; Bouloumie et al. 2002), which is defined as the accumulation of excess energy as fat in locations not classically associated with adipose tissue storage (Britton et al. 2011; Gustafson et al. 2007). Ectopic fat depots can induce both systemic (as visceral adipose tissue and intrahepatic fat) and local effects (as pericardial, myocardial and perivascular fat) (Fig. 9).

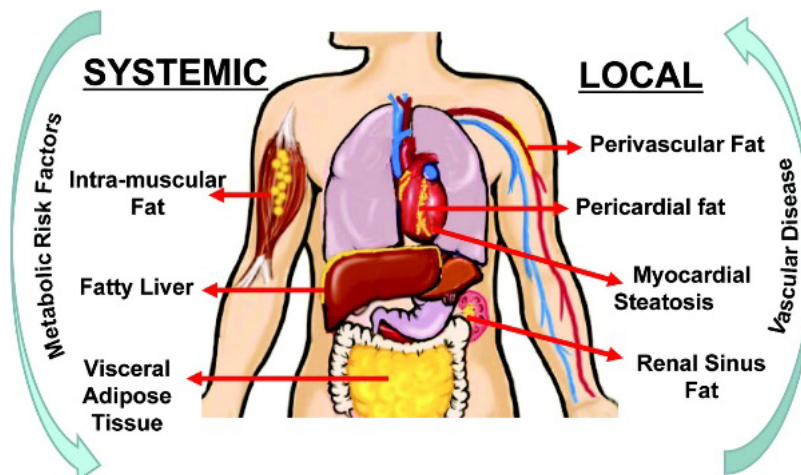


**Figure 9. Ectopic fat classification.** Ectopic fat depots in non-adipose tissues, promotes systemic and local effects, including dysfunction, insulin resistance and inflammation in the liver, muscular tissue, pancreas and visceral fat (Britton et al. 2011).

Lipids can accumulate abnormally in hepatocytes, leading to an abnormal fat accumulation in the liver that is well known as a non-alcoholic fatty liver disease (NAFLD). NAFLD is characterized by various hepatic abnormalities that ranging from hepatic steatosis to nonalcoholic steatohepatitis. This condition is extremely prevalent in obesity and is also associated with visceral adiposity (Gustafson et al. 2007). The “portal hypothesis” (Rytka et al. 2011) suggests that hepatocytes are more exposed to high levels of FFAs and inflammatory adipokines increasingly released from the visceral fat tissue into the portal vein of obese subjects. The resulting accumulation of fat in hepatocytes can lead to hepatic insulin resistance, impairment in the insulin-mediated suppression of hepatic glucose production and hence fasting hyperglycaemia (Lee et al. 2014).

The epicardial adipose tissue under normal conditions fulfills several physiologic functions, including acting as an energy source to the myocardium by releasing fatty acids (Gustafson 2010; Gustafson et al. 2007; Talman et al. 2014). However, epicardial fat may directly affect the coronary arteries and myocardium through paracrine actions of locally secreted adipokines and other bioactive molecules (Ricote et al. 1998; Tannock et al. 2004), which promote macrophage infiltration into adipose tissue, and locally reduce insulin-induced vasodilatation, leading to vasoconstriction (Chen et al. 2001).

These alterations might have long-term effects on cardiovascular function and morphology and might be responsible for cardiovascular disorders (Ricote et al. 1998).

## 1.5 Adipogenesis

Adipocytes derive from pluripotent mesenchymal stem cells (MSCs) having the capacity to develop into several cell types, including adipocytes, myocytes, chondrocytes and osteocytes. These stem cells are located in the vascular stroma of adipose tissue as well as in the bone marrow, and, when appropriately stimulated, undergo a multistep process of commitment in which the progenitor cells become restricted to the adipocyte lineage. Recruitment to this lineage gives rise to preadipocytes that then differentiate into adipocytes (Fig. 10), (Tang et al. 2012).

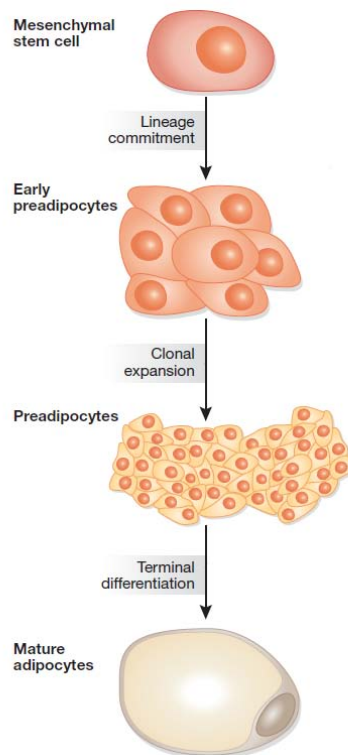


**Figure 10: Stages of adipocyte differentiation.**

*Multipotent stem cell with the capacity to differentiate along mesenchymal lineages of myoblast, chondroblast, osteoblast and adipocyte, gives rise to preadipocyte. When exposed to appropriate environmental and gene expression conditions, these cells undergo clonal expansion and subsequent terminal differentiation; cells enlarge in size while accumulating lipid vacuoles that fill the cells.*

*(Adapted from Romao et al. 2011, Ricoult et al. 2013).*

Adipogenesis can be divided into two phases: determination and terminal differentiation. Determination results in the conversion of the stem cell into a preadipocyte, which cannot be

distinguished morphologically from its precursor cell but has lost the potential to differentiate into other cell types. In the second phase, the terminal differentiation, the preadipocyte takes on the characteristics of the mature adipocyte that acquires the necessary machinery for lipid transport and synthesis, insulin sensitivity and the secretion of adipocytes-specific proteins (Rosen et al. 2006). All of these steps are controlled by a network of interacting transcription factors operating to coordinate the expression of many hundreds of proteins responsible for establishing the mature fat cell phenotype (Louet et al. 2007).

The molecular regulation of terminal differentiation is more extensively characterized than determination because of the use of cell lines that have a restricted potential to differentiate into other cell types such as 3T3L1 and 3T3-F442A murine cells.

Adipogenesis, and in particular terminal differentiation, includes a series of transcriptional processes involving the sequential expression of several transcriptional factors, culminating in the activation of CCAAT/enhancer-binding protein *C/EBPs* and *PPAR $\gamma$*  (Fig. 11).

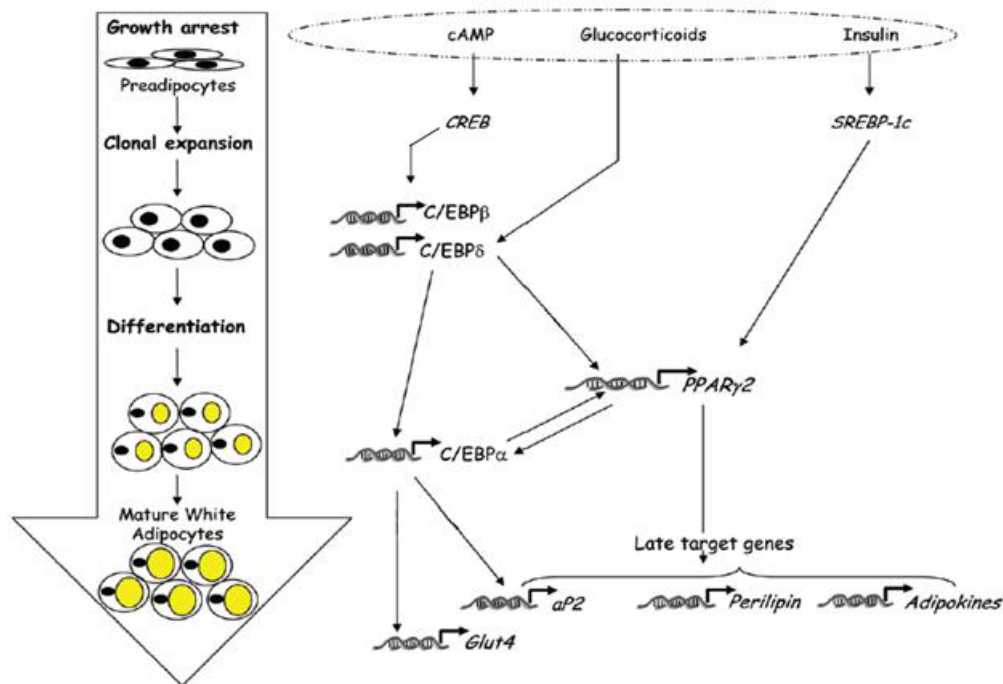


**Figure 11: A complex transcriptional cascade regulates adipogenesis.**

The transcriptional control of adipogenesis involves the activation of a variety of transcription factors. These proteins are expressed in a cascade in which *C/EBP $\beta$*  and *C/EBP $\delta$*  are among the earliest seen. These two proteins induce the expression of *PPAR $\gamma$* , which in turn activates *C/EBP $\alpha$* . *C/EBP $\alpha$*  feeds back on *PPAR $\gamma$*  to maintain the differentiated state. *ADD-1/SREBP-1* can activate *PPAR $\gamma$*  by inducing its expression as well as by promoting the production of an endogenous *PPAR $\gamma$*  ligand. All these factors contribute to the expression of genes that

*characterize the terminally differentiated phenotype. (Adapted from Louet et al. 2007; Ahmadian M et al. 2013).*

PPAR $\gamma$  is a member of the nuclear receptor super-family that plays an important role in the control of gene expression linked to a variety of physiological processes. Its most notable function is to regulate development of adipose tissue, which involves coordinating expression of many hundreds of genes responsible for the establishment of the mature adipocyte phenotype (Tontonoz et al. 1994; Evans et al. 2004; Farmer 2005).

In addition to Ppar $\gamma$ , Zfp423 was recently identified as a transcriptional regulator of preadipocyte commitment (Gupta et al. 2010). Indeed, it has been reported that the Zfp423 transcription factor is enriched in adipogenic fibroblast cell lines, relative to non-adipogenic cells. Although Zfp423 is not increased during adipogenesis, ectopic expression of Zfp423 in non-adipogenic cells is sufficient to activate Ppar $\gamma$  expression and markedly increases the adipogenic potential of these cells. Conversely, reduction of Zfp423 expression in 3T3-L1 preadipocytes or mouse embryonic fibroblasts blunts preadipocyte Ppar $\gamma$  expression and diminishes the ability of these cells to differentiate (Gupta et al. 2010).

Another important signalling pathway involved in the regulation of commitment and adipogenesis is the canonical wingless-type mouse mammary tumor virus (MMTV) integration site family (WNT) signaling pathway (Isakson et al. 2009; Logan et al. 2004). WNT family members (WNTs) are secreted glycoproteins that regulate adult tissue homeostasis and remodeling by autocrine and paracrine mechanisms (Logan et al. 2004). WNTs exert their effects by signaling through multiple so-called ‘canonical’ and ‘non-canonical’ pathways to control cell proliferation, survival, fate and behavior. Indeed, various reports have implicated WNT signaling in regulating mesenchymal stem cell proliferation, fate determination and preadipocyte differentiation (Christodoulides et al. 2009).

## **1.6 Epigenetic and adipogenesis**

Obesity results from interactions between environmental and genetic factors. Despite a relatively high heritability of obesity (40–70%), the search for genetic variants contributing to susceptibility has been a challenging task. Genome wide association (GWA) studies have identified more than 40 genetic variants associated with obesity and fat distribution. However, since these variants do not completely explain the heritability of obesity, other forms of variation, such as epigenetics marks, must be considered (Herrera et al. 2011).

Epigenetics can be defined as the study of heritable changes which affect gene function without modifying the DNA sequence (Choi et al. 2013) and could serve as a plausible link between the environment and alterations in gene expression that might lead to disease phenotypes (El-Osta et al. 2008).

Failures in imprinting are known to cause extreme forms of obesity (e.g. Prader Willi syndrome), but have also been convincingly associated with susceptibility to obesity. Furthermore, environmental exposures during critical developmental periods can affect epigenetic profile and result in obesity (Herrera et al. 2011).

Increases in adipose tissue mass and obesity are closely associated with recruitment of adipogenic transcription factors and chromatin remodeling enzyme. For example, a well-known adipogenic transcription factor, C/EBP promoter, is hypermethylated in differentiated 3T3-L1 adipocytes (Martínez et al. 2014).

Several studies have reported that epigenetic regulatory mechanisms are involved in both the commitment of pluripotent precursor cells to committed preadipocyte, and in the differentiation of preadipocytes to mature adipocytes (Musri et al. 2010). In particular, a bioinformatic analysis of the CpG islands in the promoter regions of obesity-related genes identified regions with a high density of CpGs in genes implicated in adipogenesis and inflammation such as Ppar $\gamma$ , phosphatase and tensin homolog, leptin and tumor necrosis factor  $\alpha$  (Martínez et al. 2014). Methylation of these CpG islands influences local chromatin structure and function and participates to the regulation of gene expression (Deaton et al. 2011). The role of epigenetics in adipogenesis can be explained by focusing on PPAR $\gamma$ , the master regulator of the adipocyte differentiation. Fujiki and colleagues found that the promoter of Ppar $\gamma$  gene was hypermethylated in 3T3-L1 preadipocytes, but methylation decreases during differentiation of 3T3-L1 cells and the mRNA expression increases as demethylation proceeded (Fujiki et al. 2009). In addition, also late adipogenic genes, such as insulin-responsive glucose transporter 4 (GLUT4) and leptin (LEP), are demethylated during adipogenesis, which corresponds to the expression of these genes in mature adipocytes (Pinnick et al. 2011). All together, these studies provided a high-resolution view of chromatin remodeling during cell differentiation and allowed the designation of thousands of putative preadipocyte- and adipocyte-specific cis-regulatory elements based on dynamic chromatin signatures (Martinez et al. 2014).



## 2. AIM OF THE STUDY

Hypertrophic obesity is typically associated with the development of insulin resistance and T2D. In humans, SAT hypertrophy appears to be a consequence of impaired adipocyte precursor cell recruitment into the adipogenic pathway rather than lack of precursor cells. While the underlying mechanisms have only been partially elucidated, current evidence indicates that restricted adipogenesis in SAT predicts future development of T2D independent of obesity. However, the present understanding of SAT expansion in human obesity and diabetes is limited by incomplete understanding of the molecular basis of preadipocyte determination.

Previous studies demonstrated the importance of the Ppar $\gamma$  transcriptional activator *Zfp423* in regulating preadipocyte determination and showed that *Zfp423* expression identifies committed preadipocytes. Thus, *Zfp423* is crucial for the initial formation of white adipocytes and, importantly, also plays a later role in maintaining the energy-storing phenotype of white adipose cells. Furthermore, epigenetic mechanisms have been linked to the transcriptional regulation of *Zfp423* exerted by *Zfp521*. These findings support the growing evidence that lineage determination of multipotent MSCs to the adipocyte lineage is also epigenetically regulated.

In the present work, we have investigated whether *Zfp423* is epigenetically regulated and whether these events are involved in the restricted adipogenesis in humans with expanded SAT.

Elucidation of the molecular mechanisms responsible for transcriptional regulation of *Zfp423* may improve the understanding of restricted adipogenesis in hypertrophic obesity and its unhealthy metabolic effects.

### **3. MATERIALS AND METHODS**

#### **3.1 Materials**

Media, sera, insulin, TRIzol, and SuperScript-III were from Invitrogen (San Diego, CA, USA). Rosiglitazone was from Alexis (Grünberg, Germany). 5-Azacytidine, 3-isobutyl-1-methylxanthine (IBMX) and dexamethasone (DEX) were from Sigma-Aldrich (St Louis, MO, USA). pCpGfree-Lucia was from InvivoGen (St Diego, CA, USA). SYBR-Green was from Bio-Rad (Hercules, CA, USA). DNA Methylation Kit was from Zymo Research (Orange, CA, USA). Micrococcal Nuclease, Dam<sup>-</sup>/Dcm<sup>-</sup> E.coli cells, HpyCH4IV, M.SssI, HhaI and HpaII enzymes were from New England Biolabs (Ipswich, WI, USA). DNA Purification Kit and pGEM-T-EASY Vector were from Promega (Madison, WI, USA). The PCR Purification kit was from QIAGEN (Hilden, Germany). Big Dye Terminator v3.1 Cycle Sequencing Kit was from Applied Biosystems (Foster City, CA, USA).

#### **3.2 Cell culture and adipocyte differentiation**

Mouse embryonic fibroblasts (3T3-L1 and NIH-3T3) used in this study were obtained from the American Type Culture Collection (Manassas, Virginia, USA). These mycoplasma-free cell lines were grown in DMEM with 10% foetal calf serum (FCS). For adipocyte differentiation, cells were grown to confluence in medium containing 10% FCS. Two days after reaching confluence, the cells were cultured in DMEM supplemented with a differentiation cocktail containing 5µg/ml insulin, 0.5mmol/l IBMX, 1mol/l DEX, 1 µmol/l rosiglitazone and 10% fetal bovine serum (FBS) for 2 days. Forty-eight hours after induction, cells were maintained in DMEM containing 5µg/ml insulin and 10% FBS until they were ready for collection. The NIH-3T3 cells were cultured in the presence or the absence 5-Azacytidine (5µmol/l) for 6h before the administration of differentiation cocktail. Lipid accumulation of mature adipocytes was determined by Oil Red O (ORO) staining as reported in [13]. The cells were incubated for 60 min at RT in ORO staining solution. Images were taken using an Olympus microscope system (Center Valley, PA, USA). For quantification, absorbance was measured at 510 nm using a spectrophotometer (Beckman, CA, USA).

### 3.3 Participants

This study is a secondary analysis on participants from the EUGENE2 consortium (Laakso et al. 2008). Adipose tissue derived Stromal Vascular Fraction (SVF) cells were obtained from 20 healthy non-obese individuals. Recruitment and clinical phenotyping of these individuals has been previously described (Laakso et al. 2008). The study was approved by the appropriate Institutional Review Boards. All study participants gave informed consent.

Adipose tissue biopsies were obtained from the abdominal SAT. Following careful dissection, the adipose cells were digested with collagenase for 45 minutes at 37°. After the digestion, the suspension was centrifuged to obtain two phases: an upper (mature adipocytes) and a lower phase (SVF cells). The size of adipocytes was measured according to previously described procedures (Isakson et al. 2009, Arner et al. 2011), whereas the SVF cells, in which we analysed *ZNF423* expression, were cultured in DMEM and Ham's F12 supplemented with 10% FBS and 0,002 mol/l glutamine as previously reported (Isakson et al. 2009), in order to remove the erythrocytes and inflammatory cells.

### 3.4 RNA isolation and quantitative real-time PCR

RNA was isolated by TRIzol reagent according to the manufacturer's protocol. The RT-PCR of 1µg of RNA was performed using Superscript-III. The cDNA obtained were used as a template for qRT-PCR, performed in triplicate by using iQ SYBR Green Supermix on iCycler real-time detection system (Bio-Rad). Relative quantification of gene expression is relative to the control (equal to 1) and was calculated according to the comparative method of  $2^{-\Delta\Delta CT}$  based on the threshold cycle (CT) values of the target and the housekeeping genes.

The primers used are listed in the table below (Table 2).

Gene	Forward/Reverse	Primer (5' to 3')
<i>Pparγ2</i> <i>mRNA</i>	Forward Reverse	CAGTGGAGACCGCCCAGGCT TGGAGCAGGGGGTGAAGGCT
<i>Fabp4/Ap2</i> <i>mRNA</i>	Forward Reverse	TCTCACCTGGAAGACAGCTCC GCTGATGATCATGTTGGGCTTGG
<i>Glut4</i> <i>mRNA</i>	Forward Reverse	CAGAAGGTGATTGAACAGAG AATGATGCCAATGAGAAA
<i>AdipoQ</i> <i>mRNA</i>	Forward Reverse	GTGACGACACCAAAAGGGCTC TCCAACCTGCACAAGTTCCC

<i>Cyclophilin mRNA</i>	Forward	GCAGACAAAGTTCCAAAGACAG
	Reverse	CACCCTGGCACATGAATCC
<i>Zfp423 mRNA</i>	Forward	GGTTTTATTATGTGTTTTTGTAGTGTA
	Reverse	ATATCCCTCAACTCAACCTACTTAA
<i>ZNF423 mRNA</i>	Forward	AGGCCTAGAAGGAGAGCCAG
	Reverse	TCGTCATCACCATCTCCAGG
<i>Zfp423 NUC 1 MNase</i>	Forward	CCCGCACGGGCCTGTTA
	Reverse	CTCTGACAGCACTGGGCA
<i>Zfp423 NUC 2 MNase</i>	Forward	TGTGGCCGGACGCCTG
	Reverse	CCTTCTCCTCCGCCCCTTG
<i>Zfp423 CTRL R MNase</i>	Forward	GCCCGAGGGCAGGCA
	Reverse	GCACGGGCATTGCTCAG
<i>Zfp423 Bisulfite</i>	Forward	GGTTTTATTATGTGTTTTTGTAGTGTA
	Reverse	ATATCCCTCAACTCAACCTACTTAA
<i>ZNF423 Bisulfite</i>	Forward	GAGAGGAGGAAGAAATTTAGGGTGGG GTG
	Reverse	ACTCAAAACAATCCTCAATACCTAAAA AAT

**Table 2.** List of primers used in this study.

### 3.5 Micrococcal Nuclease (MNase) protection assay

For each experiment, NIH-3T3 and 3T3-L1 cells were fixed for 10 min at 37° in growth medium by the addition of 37% (vol./vol.) formaldehyde to a final concentration of 1% (vol./vol.). The crosslinking reaction was stopped with glycine (from a 2.5 M stock) to a final concentration of 125 mM for 5 minutes at room temperature (quenches reaction). Nuclei were isolated from  $5 \times 10^5$  cells, suspended in 1 ml of wash buffer (10 mmol/l Tris-HCl (pH 7.4), 15 mmol/l NaCl, 60 mmol/l KCl and 1mmol/l CaCl<sub>2</sub>) and digested with 200 U of MNase (MNase) for 20 min at 37°. MNase digestion was stopped by adding 100 mmol/l EDTA and 10 mmol/l EGTA PH 7.5). RNA and proteins were degraded by adding of RNaseA (0,4 µg/µl), proteinase K (400 µg/ml) and NaCl (300mmol/l). Each sample was adjusted to 0.4% SDS and incubated overnight at 65° for deproteinization and crosslink reversal.

MNase digested DNA were electrophoretically separated on 1.5% agarose gel and mononucleosome-size (150 bp) bands were excised from the gel and purified by PCR clean-up

and gel extraction (Macherey-Nagel) according to the manufacturer's instructions. The purified DNA was subsequently amplified by quantitative real time RT-PCR using primers designed as follows: NUC1, NUC2 and CTRL R primer set for the Zfp423 promoter region.

### **3.6 DNA methylation assessment**

Genomic DNA from cultured cells was extracted by DNA Purification Kit (Promega). Bisulfite treatment of extracting genomic DNA was performed by EZ DNA Methylation Kit (Zymo Research), following the manufacturer's instructions. The Zfp423 promoter region in the bisulfite converted genome was amplified by PCR using Bisulfite-specific primer sets. The Bisulfite Primer Seeker software (Zymo Research) was used to design the primers for CG-rich sequences. The primers used are listed in the table 2. Converted DNA was amplified under the following conditions: 95° for 10 min and 39 cycles of 96° for 1 min, 58° for 1 min, and 72° for 2 min. For bisulfite sequencing, PCR product was cloned using pGEM T-EASY Vector system (Promega). Then, competent E.coli cells were transformed and plated on X-GAL/IPTG LB-ampicillin Agar plates, where blue colonies represent an empty vector, and white colonies represent vectors inserted with target PCR product. Ten clones from each sample were selected and plasmids containing the target DNA are extracted by using the QIAprep Spin Miniprep Kit (QIAGEN) and subjected to standard sequencing analysis, using T7 universal primer. DNA sequencing was performed on ABI 3500 Automatic Sequencer using Big Dye Terminator v3.1 (Applied Biosystems).

### **3.7 *In-vitro* methylation and luciferase reporter assay**

The 5'-flanking region of *Zfp423* gene (-1324 to -764) was amplified by PCR and cloned into pCpGfree-Lucia (InvivoGen) luciferase reporter vector. Amplification of the reporter construct was performed using Dam<sup>-</sup>/Dcm<sup>-</sup> E.coli cells (New England Biolabs). The luciferase reporter vector was *in-vitro* methylated by incubation with 1 unit/μg of M.SssI enzyme (methylates all CpG) or with 1 unit/ug of HhaI (methylates the cytosines of the sequence GCGC) and HpaII enzymes (methylates the cytosines in the sequence CCGG) at 37° for 1h. Fully methylated, unmethylated and partially methylated *Zfp423* reporter vectors were transfected in NIH-3T3. To normalise the luciferase activity, a control plasmid encoding a Renilla luciferase gene was cotransfected into the cells. After 48h, Firefly and Renilla luciferase activity were assayed using a luciferase reporter assay kit, according to the manufacturer's instructions.

### 3.8 Site-direct mutagenesis and luciferase reporter assay

*Zfp423* promoter (-1037/-1002) was amplified by PCR and cloned into the Firefly luciferase reporter pCpGfree-promoter-Lucia vector (Invivogen). One-step polymerase chain reaction-based mutagenesis technique was used to generate site-specific mutation and to produce mutated construct (mut). One complementary pair of primers was designed that contained the desired mutation, replacing the cytosine at -1016 position with adenine. Both the wt and mut constructs were transformed into E.coli GT115 cells (Invivogen). *In-vitro* methylation was performed using the M.SssI methyltransferase following manufacturer's protocol (New England BioLabs). Unmethylated wt and mut constructs were obtained in the absence of M.SssI. Methylation was confirmed by resistance to HpyCH4IV digestion (New England BioLabs). After 48h, Firefly and Renilla luciferase activity were assayed using a luciferase reporter assay kit, according to the manufacturer's instructions.

### 3.9 Statistical analysis

All experiments were performed three times for each determination and are shown as means  $\pm$  SD. *P*-values between data sets were determined by two-tailed, unpaired Student's t-test. Significant probability (*p*)-values are indicated as \*\*\**p*<0.001, \*\**p*<0.01 and \**p*<0.05. Correlation analysis was calculated using Pearson's correlation coefficient.

## 4. RESULTS

### 4.1 Promoter methylation reduces *Zfp423* expression in NIH-3T3 cells

Based on the aims above described, the experiments were performed in two cellular models with a different adipogenic capability; the 3T3-L1 cells, which are fibroblasts committed to adipocyte lineage, widely used to study *in vitro* adipogenesis; and the NIH-3T3 cells, which are fibroblasts with a reduced adipogenic capability and generally used as negative controls for *in-vitro* adipogenesis.

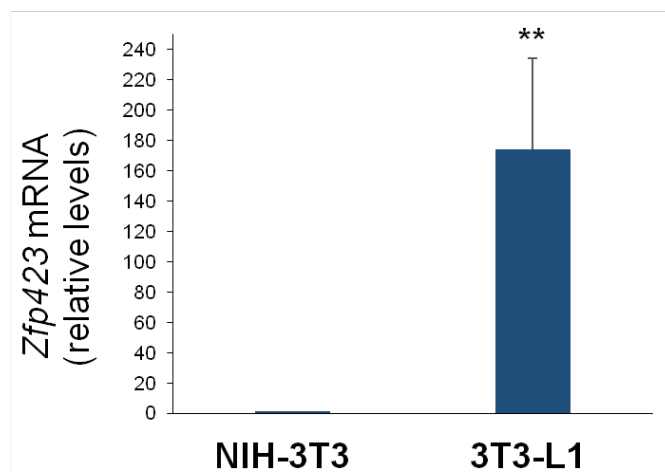
The mRNA expression of *Zfp423* genes was evaluated by quantitative real time RT-PCR (qRT-PCR) and found it to be barely detectable in the NIH-3T3 and highly expressed in the 3T3-L1 cells ( $p<0.01$ ) (Fig. 1a).

Importantly, there was no sequence variation of the *Zfp423* promoter in NIH-3T3 and 3T3-L1 cells (data not shown), suggesting that the differential expression observed had not to be attributed to the DNA sequences of its promoter, but this remain to be investigated.

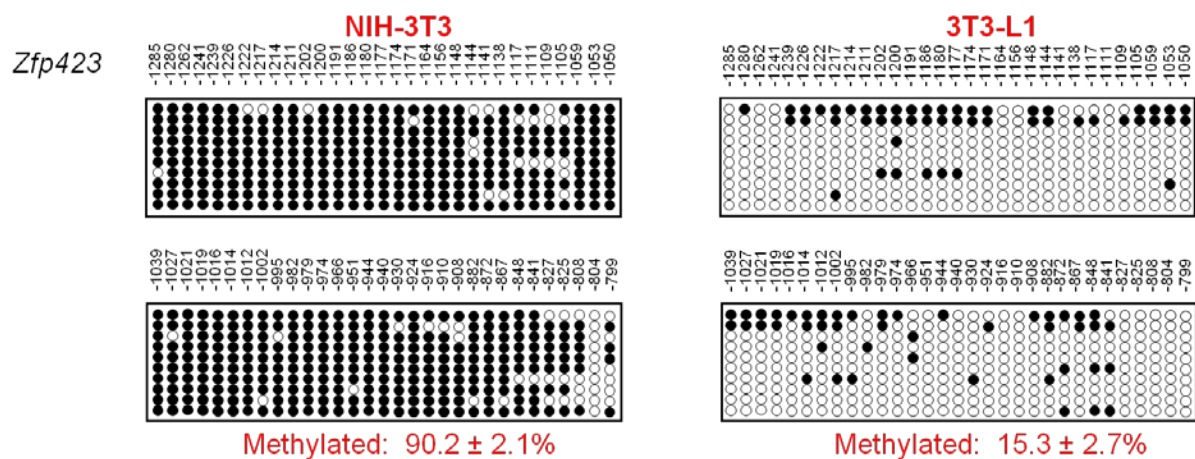
Then, to understand the reasons at the basis of the decreased *Zfp423* expression observed in NIH-3T3 cells, the contribution of DNA methylation in the transcriptional regulation was examined and the specific methylation status of the promoter was determined *in-vitro* with appropriate experimental procedures in both NIH-3T3 and 3T3-L1 cells. We subjected the *Zfp423* promoter region to bioinformatic analysis. EMBOSS CpGplot revealed a large 560bp CpGi upstream *Zfp423* transcription start site (TSS), providing a potential basis for methylation control of *Zfp423* expression. We analysed the methylation status of the *Zfp423* CpGi by bisulfite sequencing in both NIH-3T3 and 3T3-L1 cells and found massive demethylation in the latter cell type (15.3% vs. 90.2% in NIH-3T3 cells;  $p<0.001$  Fig. 1b).

The causal relationship between the methylation status of the *Zfp423* promoter and its mRNA expression was then evaluated by cloning the *Zfp423* promoter region into a luciferase reporter (pCpGfree-Lucia) vector, which was completely methylated by M.SssI enzyme, or partially methylated by HhaI and HpaII enzymes, or not methylated. Methylation status of these vectors was confirmed by digestion with HpyCH4IV, a methylation-sensitive restriction enzyme (data not shown). As shown in Fig. 1c, Luciferase activity in the constructs harboring the fully and the partially methylated *Zfp423* promoters declined, respectively, by 80 and 40% compared to the unmethylated promoter ( $p<0.001$ ). These results demonstrate that methylation regulates *Zfp423* promoter function *in-vitro*.

**a**



**b**



**c**

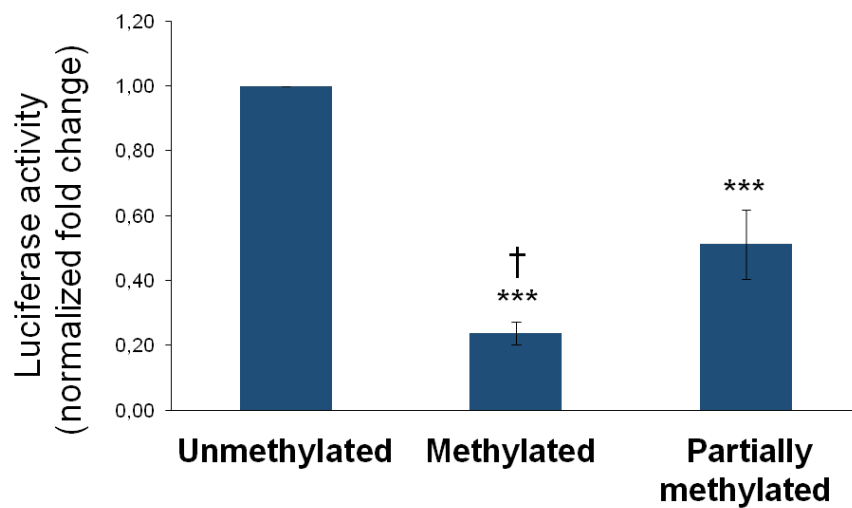


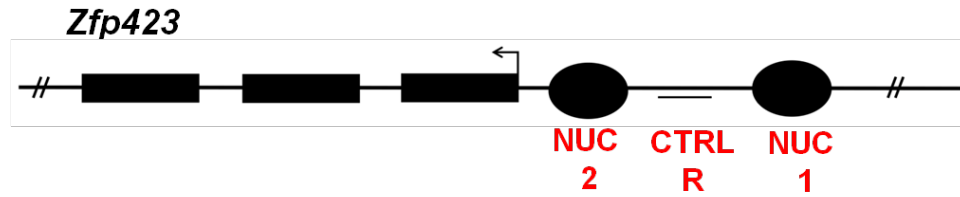


**Figure 1. Zfp423 mRNA expression and promoter methylation in NIH-3T3 and 3T3-L1 cells.** (a) Total RNA was isolated from the cells and Zfp423 mRNA levels were assessed by qRT-PCR. Data normalization was achieved using the housekeeping Cyclophilin gene as internal control. Results are the means  $\pm$  SD from three independent experiments. Statistical significance was tested by 2-tail Student's t-test (\*\* $p < 0.01$ ). (b) Bisulfite sequencing analysis and assessment of Zfp423 promoter methylation of individual methylated CpG sites were compared in NIH-3T3 and 3T3-L1 cells [Methylation:  $90.2 \pm 2.1\%$  NIH-3T3;  $15.3 \pm 2.7\%$  3T3-L1]. Each PCR product was sub-cloned and ten clones were analyzed by bisulfite sequencing. Individual CpG sites at the Zfp423 promoter, either methylated (filled circles) or unmethylated (open circles), were aligned to their sequence position as indicated on top of the panels. Results are the means  $\pm$  SD from three independent experiments. Statistical significance was tested by 2-tail Student's t-test ( $p < 0.001$ ). (c) Luciferase activity of the in-vitro unmethylated, methylated, or partially methylated Zfp423 promoter reporter constructs in NIH-3T3 cells. Relative Luciferase activity was normalized against the activity of a cotransfected internal vector. Results are the means  $\pm$  SD of three independent experiments. Statistical significance was tested by 2-tail Student's t-tests (\*\*\* $p < 0.001$  vs. unmethylated vector, and † $p < 0.05$  vs. partially methylated vector).

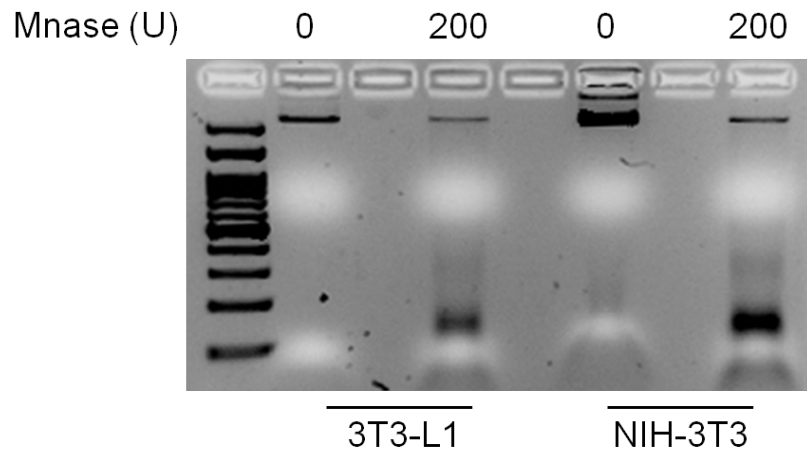
## 4.2 Nucleosome occupancy of Zfp423 promoter is increased in NIH-3T3 compared to 3T3-L1 cells

To test whether the differences in Zfp423 gene expression, found in NIH-3T3 and 3T3-L1 cells, may be linked to different nucleosome occupancy of the gene promoter, the genomic sequence was analyzed by the bioinformatic tool NuPoP. Based on bioinformatics analysis, Zfp423 promoter exhibits several potential regions where nucleosome positioning featured high prediction score (Fig. 2a); suggesting that differential Zfp423 expression in NIH-3T3 and 3T3-L1 cells is also accompanied by variation in nucleosome occupancy. To validate this hypothesis and assess nucleosome occupancy at the best-predicted regions, MNase protection assay was performed and nucleosome positioning checked in mono-nucleosomal DNA by qRT-PCR (Fig. 2b). Percentage of nucleosome occupancy at two such regions of the Zfp423 promoter was significantly higher in NIH-3T3 cells (NUC1 % occupancy: 72.2 vs. 51.5 in 3T3-L1 cells;  $p < 0.01$ . NUC2 % occupancy: 94.6 vs. 46.4 in 3T3-L1 cells;  $p < 0.001$ ; Fig. 2c). No significant difference was observed in the CTRL region, where nucleosome positioning featured low bioinformatic prediction score. Thus, in these cells, nucleosome occupancy of the promoter inversely correlates with Zfp423 expression suggesting that dynamic chromatin remodeling may also contribute to transcriptional regulation.

**a**



**b**



**c**

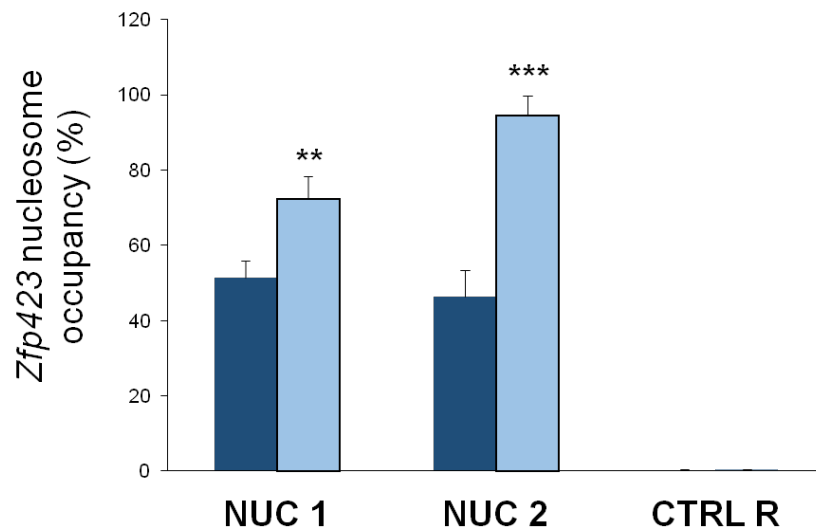


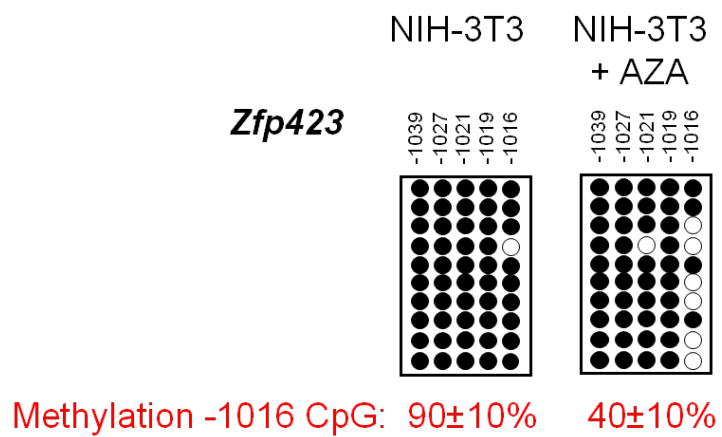
**Figure 2. Nucleosome occupancy at Zfp423 promoter in 3T3-L1 and NIH-3T3 cells. (a)** Schematic representation of the regions potentially occupied by nucleosomes at the Zfp423 promoter in NIH-3T3 and 3T3-L1 cells. Genomic position: NUC1 chr8:87,960,746-87,960,945; NUC2 chr8:87,959,646-87,959,845; CTRL Reg chr8:87,960,121-87,960,322. **(b)**

*Genomic DNA was obtained by lysis of 3T3-L1 and NIH-3T3 cell nuclei and either digested with MNase or untreated. (c) The percentage of nucleosome occupancy at two bioinformatically-identified regions of the Zfp423 promoter (NUC1 and NUC2) and in negative control region (CTRL R) was assessed by qRT-PCR. Nucleosome occupancy across the analysed region was quantified by the  $2^{-\Delta CT}$  method using the undigested input as normalising control. Dark blue bars represent 3T3-L1 cells; light blue bars represent NIH-3T3 cells. Results are the means  $\pm$  SD from three independent experiments. Statistical significance was tested by 2-tail Student's t-tests (\*\* $p < 0.01$ , and \*\*\* $p < 0.001$  vs. 3T3-L1 cells.*

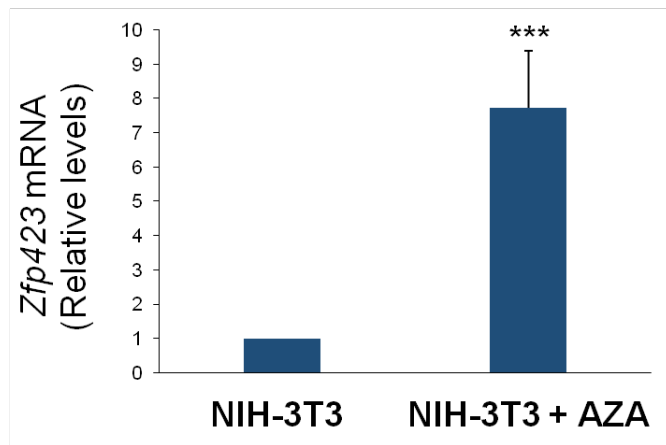
### **4.3 5-Azacytidine enhances Zfp423 expression and allows differentiation of non-adipogenic NIH-3T3 cells**

To assess whether DNA methylation regulates Zfp423 expression also in intact cells, we investigated the ability of the DNA methyltransferase inhibitor 5-Azacytidine (AZA) to remove the transcriptional block imposed on Zfp423 in the NIH-3T3 cells. Incubating the cells with AZA mainly affected the methylation level at CpG position -1016 (40% methylation in exposed vs. 90% in unexposed cells;  $p < 0.01$ ; Fig. 3a) and this was associated with a 6-fold increase in Zfp423 mRNA expression ( $p < 0.01$ ; Fig. 3b). However, besides the -1016 CpG, the overall methylation profile at Zfp423 promoter does not change in AZA treated cells (data not shown), providing a potential explanation for why mRNA expression levels are still lower compared to 3T3-L1 cells. Nevertheless, MNase protection studies revealed that AZA significantly reduced nucleosome occupancy at the NUC1 and NUC2 regions ( $p < 0.001$ ; Fig. 3c), further underlining the potential role of chromatin remodelling of the Zfp423 regulatory region in transcriptional regulation.

**a**



**b**



**c**

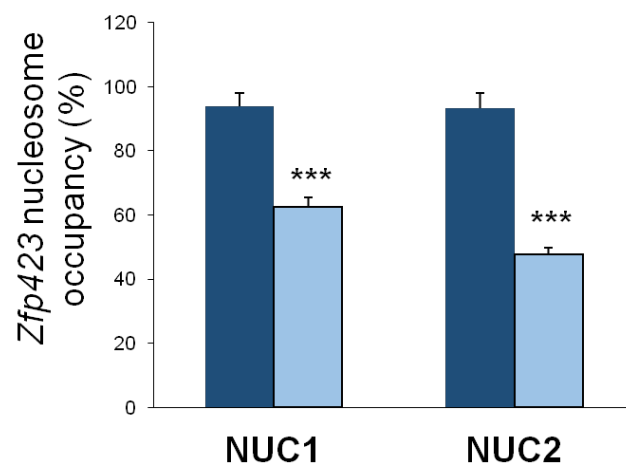
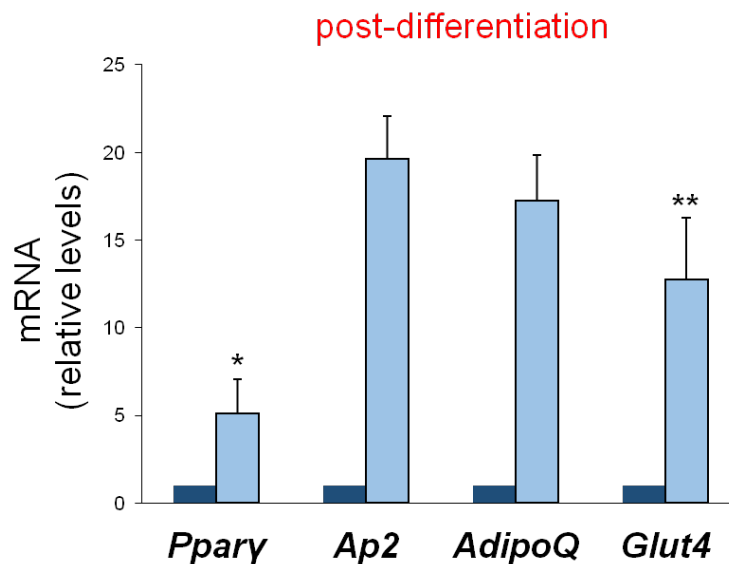


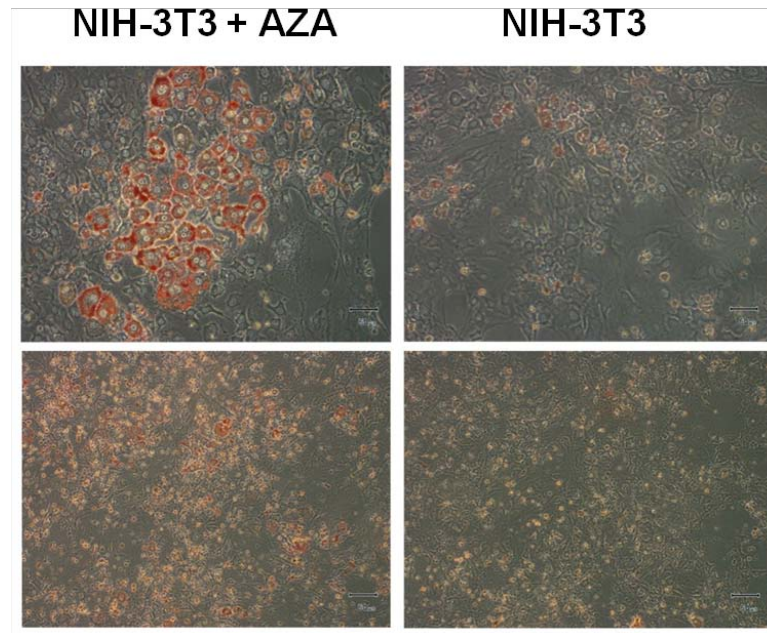
**Figure 3. Effect of 5-Azacytidine on Zfp423 mRNA expression and nucleosome occupancy in NIH-3T3 cells.** Cells were cultured in medium supplemented with AZA. (a) Bisulfite sequencing analysis of the DNA methylation and percentages of methylated -1016 CpG positions in Zfp423 promoter in NIH-3T3 and NIH-3T3+AZA cells [Methylation -1016 CpG:  $90 \pm 10\%$  NIH-3T3;  $40 \pm 10\%$  NIH-3T3+AZA]. Each PCR product was sub-cloned and ten clones were analysed by bisulfite sequencing. The methylation profile of each CpG site in the Zfp423 promoter, either methylated (filled circles) or unmethylated (open circles), is aligned corresponding to its sequence position. Results are the means  $\pm$  SD from three independent experiments. Statistical significance was tested by 2-tail Student's t-test ( $p < 0.01$ ). (b) Expression of Zfp423 mRNA was then measured by qRT-PCR in NIH-3T3 and NIH-3T3+AZA cells. Data normalisation has been achieved using the housekeeping Cyclophilin gene as internal control. Results are the means  $\pm$  SD from three independent experiments. Statistical significance was analysed by 2-tail Student's t-test (\*\* $p < 0.01$ , and \*\*\* $p < 0.001$  vs. NIH-3T3 cells). (c) The percentage of nucleosome occupancy was analysed by qRT-PCR in the two previously identified NUC1 and NUC2 regions of the Zfp423 promoter. The assessment has been performed in the absence (dark blue bars) or in the presence (light blue bars) of 5-Azacytidine. Results are the means  $\pm$  SD from three independent experiments. Statistical significance was tested by 2-tail Student's t-tests (\*\*\* $p < 0.001$  vs. NIH-3T3).

In parallel, AZA robustly enhanced expression of *Ppar $\gamma$*  and the differentiation markers *Ap2/Fabp4*, *AdipoQ*, and *Glut4* after induction of differentiation (Fig. 4a), accompanied by >2-fold increased cytoplasmic accumulation of Oil Red O staining (ORO) (Fig. 4b, 4c). Thus, in parallel with transcriptional activation, *Zfp423* promoter demethylation by AZA also promoted differentiation of the non-adipogenic NIH-3T3 cell line.

**a**



**b**



**c**

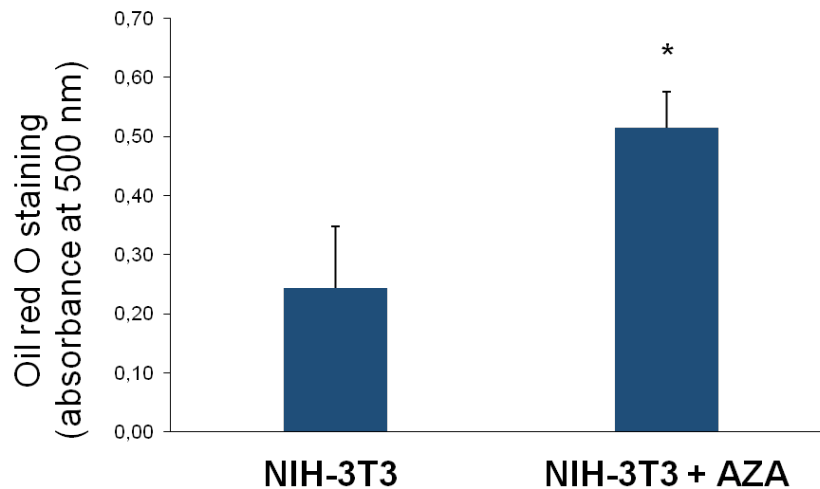


**Figure 4. Effect of 5-Azacytidine on NIH-3T3 cell adipogenic differentiation.** Cells were cultured in the presence (light blue bars) or the absence (dark blue bars) of AZA. Gene expression and lipid accumulation were assessed eight days upon the induction of adipocyte differentiation. (a) The relative mRNA levels of *Ppar $\gamma$* , *Ap2/Fabp4*, *AdipoQ* and *Glut4* were determined by qRT-PCR. Data normalization has been performed using the housekeeping *Cyclophilin* gene as internal control. Results are the means  $\pm$  SD of three independent experiments. Statistical significance was established by 2-tail Student's t-test (\* $p < 0.05$ ,

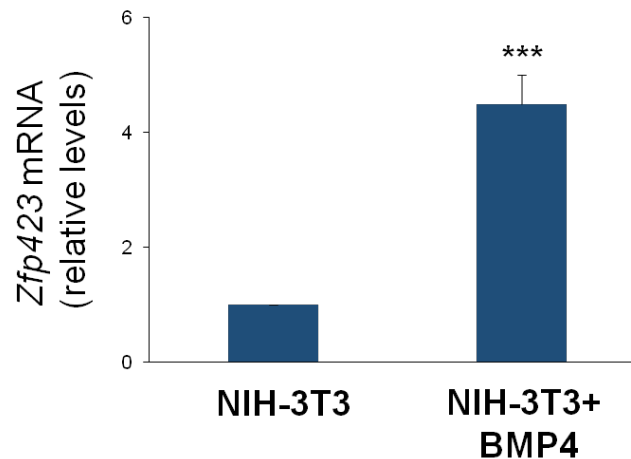
**\*\* $p < 0.01$ , and \*\*\* $p < 0.001$ ). (b)** At day 8, cells were fixed and stained with ORO. Representative microphotographs are shown at two different magnifications (20X, 10X). **(c)** Quantification of ORO staining. Results are the means  $\pm$  SD of three independent experiments. Statistical significance was tested by 2-tail Student's *t*-tests (\* $p < 0.05$  vs. NIH-3T3).

#### 4.4 BMP4 promotes *Zfp423* expression by inducing promoter demethylation

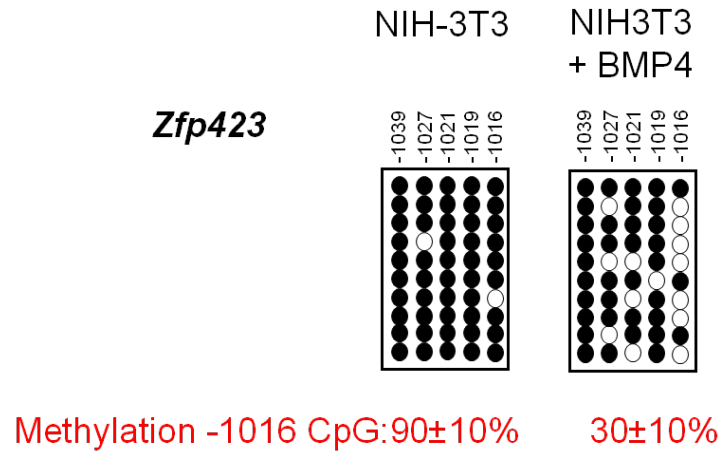
BMPs are members of the TGF-superfamily that play a key role in inducing adipocyte precursor cell commitment towards the adipogenic lineage but the molecular details of their action have been only partially elucidated. We found that adding BMP4 to the culture medium of NIH-3T3 cells enhanced the expression of *Zfp423* by almost 5-fold ( $p < 0.001$ , Fig. 5a). As revealed by bisulfite sequencing, this BMP4-dependent change was accompanied by an almost 3-fold reduced methylation at position -1016 in the *Zfp423* promoter ( $p < 0.01$ ), reminiscent of that observed upon 5-Azacytidine treatment (Fig. 5b).

We, therefore, aimed at establishing the functional significance of the -1016 dinucleotide for *Zfp423* promoter function by site-directed mutagenesis. After replacement of the cytosine at position -1016 with adenine, the 35bp fragment (-1037 to -1002) of the *Zfp423* promoter was cloned in a Luciferase reporter vector (pCpGfree-promoter-Lucia). Luciferase activity was subsequently assayed in NIH-3T3 cells transfected with either the *in-vitro* methylated or the unmethylated promoter. As shown in Fig. 5c, the -1016 mutation did not affect activity of the unmethylated *Zfp423* promoter. However, the mutation abolished the effect of methylation on promoter silencing, indicating that the -1016 dinucleotide modulates *Zfp423* transcription *in-vitro*.

**a**



**b**



**c**

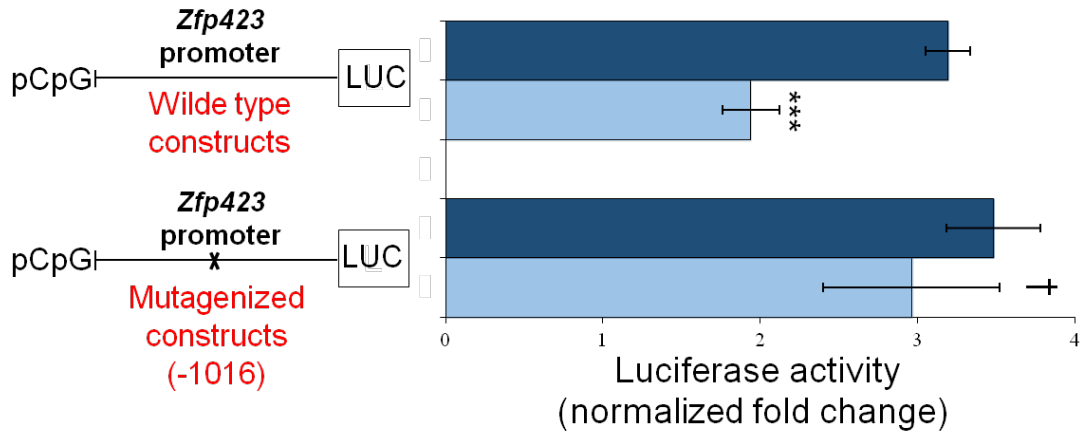


**Figure 5. Effect of BMP4 on Zfp423 mRNA expression and promoter methylation in NIH-3T3 cells.** Cells were cultured in medium supplemented with 50ng/ml BMP4. (a) Expression of Zfp423 mRNA was measured by qRT-PCR. Results are the means  $\pm$  SD from three independent experiments. Statistical significance was analysed by 2-tail Student's t-test ( $***p < 0.001$  vs. NIH-3T3). (c) Bisulfite sequencing analysis of the DNA methylation status and percentage of the methylated -1016 CpG position at the Zfp423 promoter in NIH-3T3 cells upon exposure to BMP4 [Methylation -1016 CpG: 90 $\pm$ 10% NIH-3T3; 30 $\pm$ 10% NIH-3T3+BMP4]. Each PCR product was sub-cloned and ten clones were analysed by bisulfite sequencing. The methylation profile of each CpG site at the Zfp423 promoter, either methylated (filled circles) or unmethylated (open circles), is aligned corresponding to their sequence position. Results are the means  $\pm$  SD from three independent experiments. Statistical significance was tested by 2-tail Student's t-test ( $p < 0.01$ ). (c) Effect of mutagenesis at the -1016 CpG position on Zfp423 promoter. Disruption of CpG was performed by site-directed



*mutagenesis as described under Methods. Wild-type and mutated plasmids were treated with DNA-methylase M.SssI and transfected into NIH-3T3 cells (light blue bars). Dark blue bars represent the untreated plasmids. Luciferase Activity was normalised to Renilla luciferase activity. Error bars represent SD from three replicates. Statistical significance was tested by 2-tail Student's *t*-tests (\*\**p*<0.001 vs. wild type unmethylated, and <sup>†</sup>*p*<0.05 vs. wild type methylated).*

#### **4.5 Preadipocyte *ZNF423* expression correlates with mature subcutaneous adipose cell size in humans.**

To explore the significance of *Zfp423* expression in human adipose tissue development and function, we first analysed transcription of human *ZNF423* (human ortholog of *Zfp423*) (Harder et al. 2013) in preadipocytes from the SVF of 20 healthy non-obese individuals. Participants were recruited as described in (Laakso et al. 2008) and their clinical features are presented in Table 1.

	Mean ± SD
<i>N</i>	20
<i>Age, years</i>	40.8 ± 7.9
<i>BMI, Kg/m<sup>2</sup></i>	25.4 ± 2.6
<i>Fat percent, %</i>	26.0 ± 6.7
<i>Free Fat Mass, Kg</i>	57.4 ± 10.4
<i>Cell size, µm</i>	95.9 ± 9.5
<i>GIR/bw, mg/min</i>	9.1 ± 3.1
<i>f-insulin, pmol/l</i>	348 ± 179.4
<i>fb-glucose, mmol/l</i>	4.6 ± 0.5
<i>OGTT p-glucose 2h, mmol/l</i>	6.1 ± 1.8

**Table 1.** *Clinical characteristics of the study group.*

Notably, subcutaneous adipose cell size varies over a broad range even in these non-obese individuals which is consistent with different adipogenic potential of the precursor cells. *ZNF423* mRNA was well detectable in the cells from all and, importantly, expression in the preadipocytes exhibited a significant negative correlation with the size of the mature subcutaneous adipose cells from these same individuals (Fig.6; *r* = -0.5258, *p*<0.05). This

finding shows that low *ZNF423* expression in the adipose precursor cells is a marker of subcutaneous adipocyte size of the donors and, thus, adipogenesis and the development of inappropriate adipose cell hypertrophy and associated insulin-resistant phenotype.

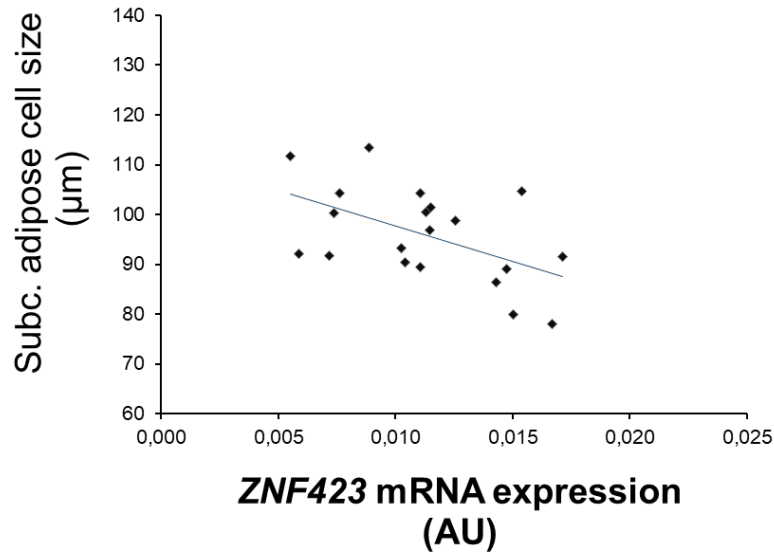


**Figure 6. *ZNF423* expression in preadipocytes from non-obese individuals with different subcutaneous adipocyte size.** *ZNF423* mRNA expression was quantitated in preadipocytes obtained from the SVF of SAT in  $n=20$  healthy non-obese individuals as described under Methods. Correlation was assessed by linear regression analysis (*ZNF423*:  $r = -0.525$ ).

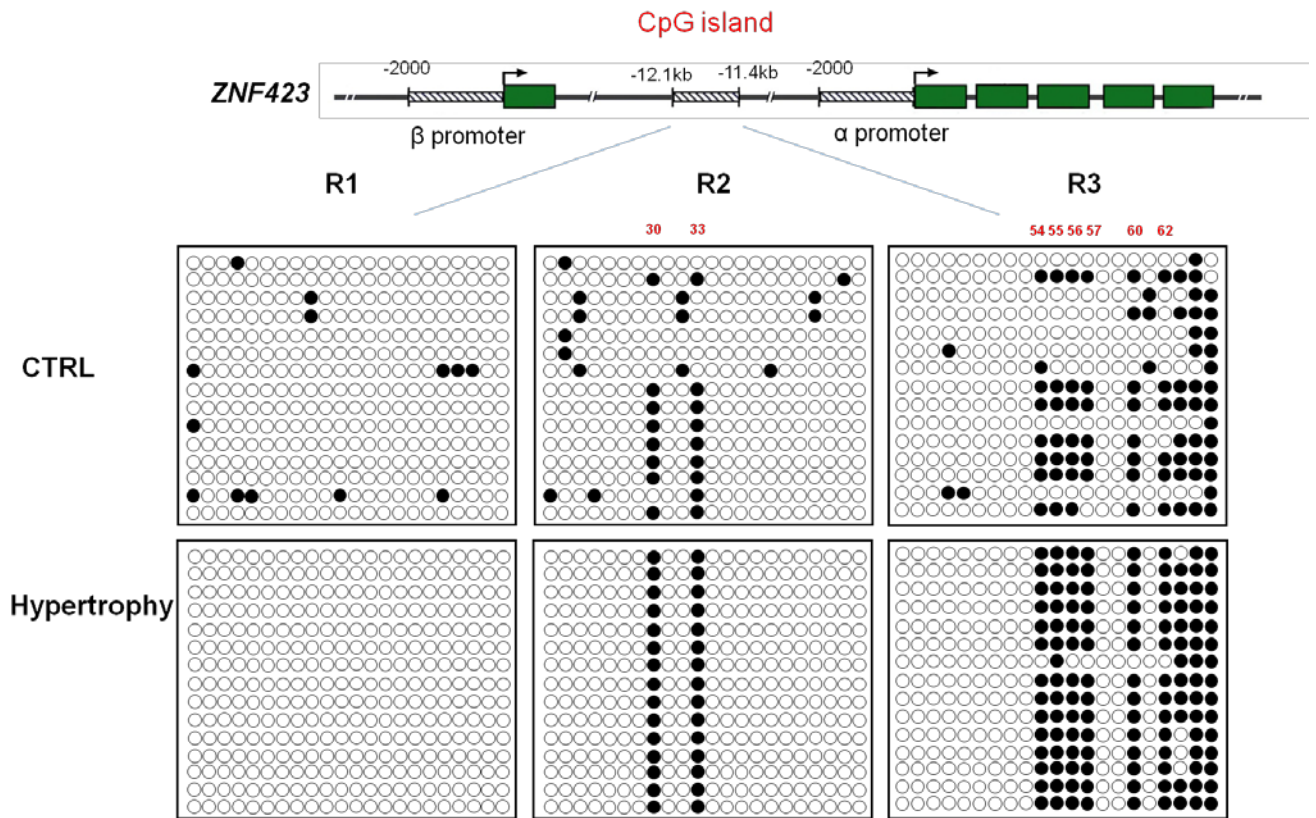
The central enhancer CpGi at the human *ZNF423* locus features >80% homology in mammals (Harder et al. 2013) and, based on site-specific mutagenesis studies in leukemia cells, was shown to be relevant for the functional regulation of both  $\alpha$  and  $\beta$  *ZNF423* promoters (Harder et al. 2013). In human preadipocytes, we observed that *ZNF423* $\alpha$  is the predominant isoform while *ZNF423* $\beta$  is barely detectable (data not shown).

To further explore the mechanisms determining *ZNF423* expression in the SVF preadipocytes, we performed bisulfite sequencing of the entire enhancer CpGi in three individuals featuring the smallest size in their subcutaneous adipocytes and an equal number of individuals exhibiting the largest adipocyte size. All of these individuals were non-obese and had similar BMI. This analysis revealed massively increased methylation levels at two sub-regions of the CpG enhancer island in these latter individuals (Fig. 7a). Indeed, the R2 sub-region featured >90% methylation at CpG dinucleotides 30 and 33 in the participants with subcutaneous adipocyte hypertrophy, compared to <20% in those featuring smaller adipocytes, respectively

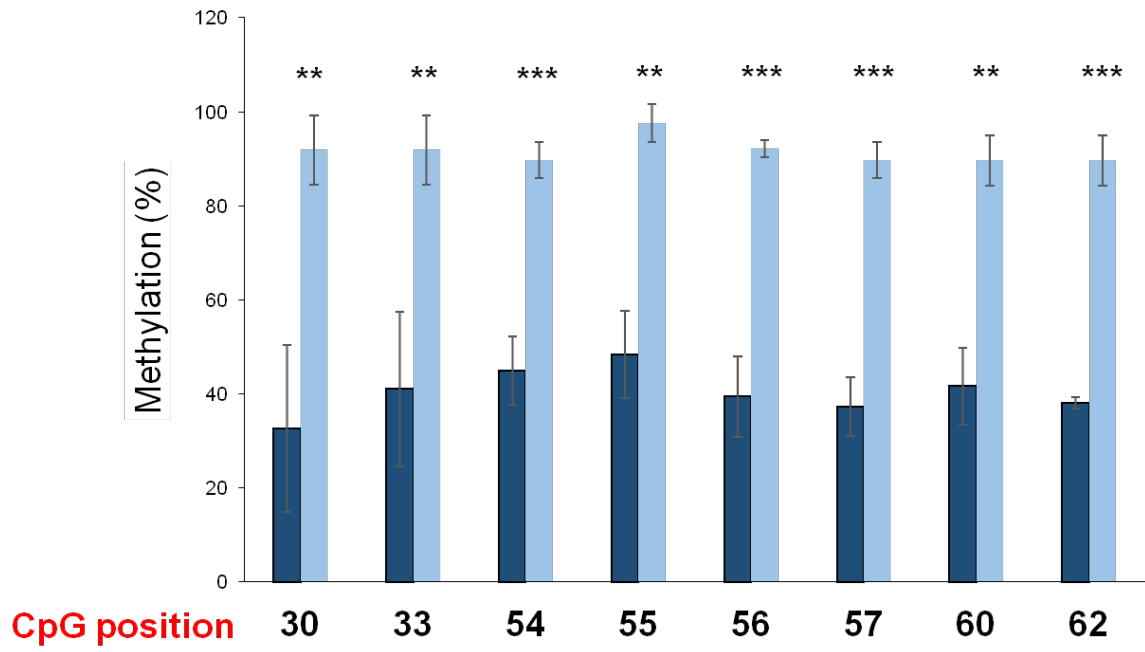
(Fig. 7b). Similarly, the R3 sub-region revealed >90% and <45% methylation at CpG nucleotides 54-57, 60, 62 respectively, in the individuals with and without adipose cell hypertrophy. In addition, AZA treatment of preadipocytes isolated from individuals with adipose cell hypertrophy led to >2-fold increased *ZNF423* expression (Fig. 7c). AZA strongly decreased the methylation level at CpG positions 54-57, 60, 62 of the R3 sub-region, consistent with the important role of these CpG in regulating *ZNF423* expression (Fig. 7d). Methylation at regions R1 and R2 was not affected by AZA (data not shown).

Taken together, these data indicate a non-permissive transcriptional state at the *ZNF423* locus in the SVF precursor cells from individuals who develop inappropriate subcutaneous adipose cell hypertrophy, a marker of impaired adipogenesis.

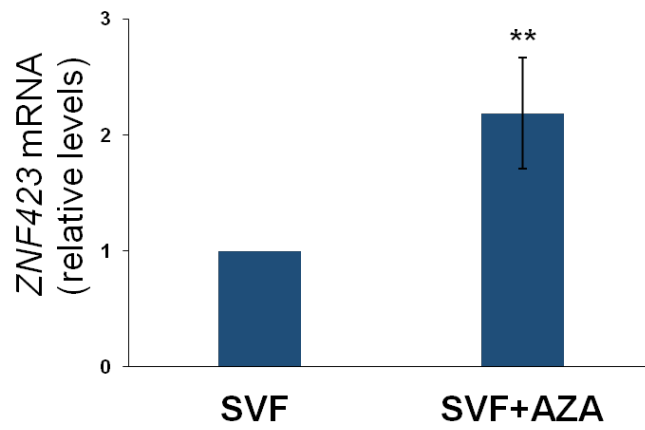
**a**



**b**



**c**



d

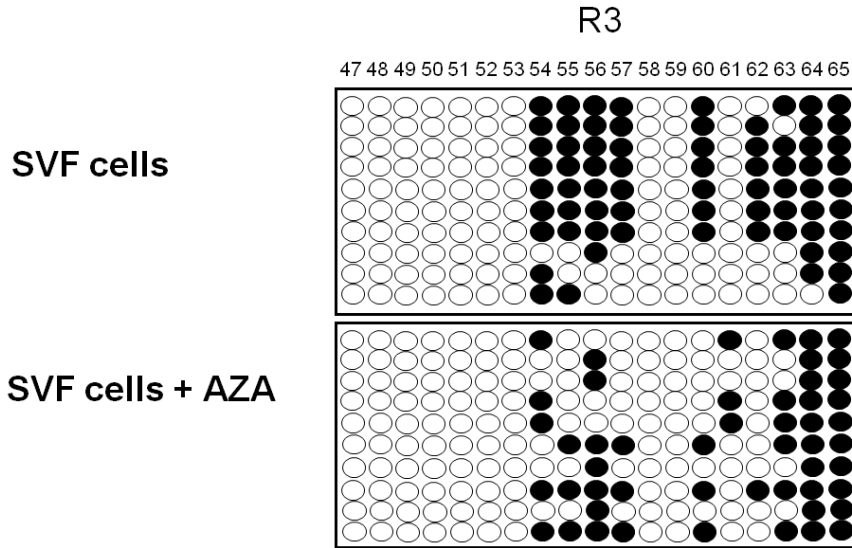


**Figure 7. DNA methylation at the *ZNF423* promoter in SVF cells from non-obese individuals with subcutaneous adipocyte hypertrophy.** Genomic DNA from preadipose SVF cells was obtained from n=3 of the individuals analysed in Fig. 6 and exhibiting the most extreme subcutaneous adipocyte hypertrophy (Hypertrophy) and n=3 individuals featuring the lower adipocyte size (CTRL). The individual DNA preparations were exposed to bisulfite as described under Methods and individually analysed by PCR amplification of the CpGi at the *ZNF423* enhancer region (-12.1 Kb; -11.4 Kb). PCR products were then individually subcloned and sequenced. (a) Methylation of 65 CpGs at the three *ZNF423* promoter regions termed R1-R3 is shown for fifteen replica clones. Open and filled circles indicate unmethylated and methylated CpGs, respectively. A representative experiment with one individual featuring SAT hypertrophy (hypertrophy) and one control individual is shown (n=3). (b) Quantification of the methylation levels at eight specific CpGs in individuals featuring the smallest size in their subcutaneous adipocytes (dark blue bars) and in individuals exhibiting the largest adipocyte size (light blue bars). Error bars represent SD from three individuals per group. Statistical significance was tested by 2-tail Student's t-tests (\*\* $p < 0.01$ , and \*\*\* $p < 0.001$ ). (c) Expression of *ZNF423* mRNA was measured by qRT-PCR. Results are the means  $\pm$  SD from three independent experiments. Statistical significance was analysed by 2-tail Student's t-test (\*\* $p < 0.01$  vs. SVF cells). (d) Methylation at the R3 region on *ZNF423* promoter is shown for ten replica clones. Open and filled circles indicate unmethylated and methylated CpGs, respectively. A representative experiment of three individual experiments with AZA treated/untreated SVF cells from one individual featuring SAT hypertrophy (hypertrophy).

## 5. DISCUSSION

Previous studies demonstrated the importance of the *Ppar $\gamma$*  transcriptional activator *Zfp423* in regulating preadipocyte determination (Gupta et al. 2010) and showed that *Zfp423* expression identifies committed preadipocytes (Gupta et al. 2012). Thus, *Zfp423* is crucial for the initial formation of white adipocytes and, importantly, also plays a later role in maintaining the energy-storing phenotype of white adipose cells (Shao et al. 2016). Moreover, epigenetic mechanisms have been linked to the transcriptional regulation of *Zfp423* exerted by ZFP521. ZFP521 binds the promoter and intronic regions of *Zfp423* and represses its expression by promoting histone modifications. These findings support the growing evidence that lineage determination of multipotent MSCs to the adipocyte lineage is also epigenetically regulated (Addison et al. 2014).

Given the central role of *Zfp423* in controlling preadipocyte commitment, in this study we investigate whether *Zfp423* gene is under epigenetic regulation and if this plays a role for the early induction of adipogenesis. To this aim, we carried out our study in 3T3-L1 and NIH-3T3 cells, which are respectively adipocyte lineage committed and non-adipogenic fibroblasts (Fujiki et al. 2009).

In this study, we show that *Zfp423* is transcribed in 3T3-L1 preadipose cells but not in NIH-3T3 non-preadipose fibroblasts. Furthermore, we identified a large CpGi at the *Zfp423* promoter and report, for the first time, that *Zfp423* expression in 3T3-L1 cells is accompanied by an extensive demethylation of this *Zfp423* region, followed by decreased nucleosome occupancy.

This finding implicated a causal relationship between the different epigenetic profile and *Zfp423* transcription in 3T3-L1 and NIH-3T3 cells. Consistent with this hypothesis, we found no DNA sequence variation at the *Zfp423* promoter in the two cell types. Luciferase assays provided formal proof that methylation directly represses *Zfp423* promoter function *in-vitro*. In addition, exposure to the demethylating agent 5-Azacytidine simultaneously caused *Zfp423* promoter demethylation and rescued *Zfp423* transcription in intact NIH-3T3 fibroblasts. Thus, promoter methylation is an important regulator of the differential transcription of *Zfp423* in non-preadipose and preadipose fibroblasts.

DNA methylation inhibits gene expression by at least two mechanisms. Firstly, cytosine methylation may directly inhibit the association of DNA binding factors (Fujiki et al. 2009, Klose et al. 2006). Secondly, proteins that recognize methylated CpG sites may recruit transcriptional corepressor molecules, including histone modification and chromatin remodelling enzymes, and cause a transcriptionally repressed chromatin state (Fujiki et al. 2009, Klose et al. 2006). In our work, MNase digestion assays revealed that, in the preadipose

3T3-L1 fibroblasts, the CpG demethylation of the *Zfp423* promoter is accompanied by nucleosome repositioning in an open chromatin state which may contribute to *Zfp423* active transcription. The ability of 5-Azacytidine to induce this same nucleosome repositioning suggests that, in the NIH-3T3 cells, demethylation of the *Zfp423* promoter may trigger chromatin remodelling in a transcriptionally active conformation, thereby inducing *Zfp423* expression. Therefore, while direct association of transcriptionally relevant DNA binding factors to methylated cytosines was not investigated in this work, CpG methylation-triggered chromatin condensation appears to be an important mechanism for maintaining the methylated *Zfp423* promoter silenced.

Previous studies demonstrated that *Zfp423* transcription is essential for preadipocyte commitment, enabling further adipogenic differentiation (Gupta et al. 2010, Gupta et al. 2012). In line with this, we show that the effect of 5-Azacytidine on *Zfp423* promoter epigenetics and active gene transcription was followed by rescue of the differentiation capacity of the NIH-3T3 fibroblasts as revealed by a robust raise in *Ppar $\gamma$* , *Ap2/Fabp4*, *AdipoQ* and *Glut4* levels. ORO accumulation in NIH-3T3 cytoplasm was also increased following exposure to 5-Azacytidine. Therefore, in the model we now propose, commitment of an adipocyte precursor cell is accompanied by the acquisition of a specific chromatin epigenetic signature of the *Zfp423* locus (Gupta et al. 2010, Bell et al. 2011). Importantly, as shown in this work, these events appeared to be reversible. Indeed, the exposure of the uncommitted NIH-3T3 cell to an epigenetic agent, i.e., 5-Azacytidine, reprogrammed in part the epigenetic signature at the *Zfp423* promoter, favouring commitment and adipogenesis. However, 5-Azacytidine does not make the NIH-3T3 cells an *in-vitro* model of spontaneous adipogenesis (data not shown). This is not surprising because *Zfp423*, identified as a major determinant of preadipocyte commitment, is not responsible for the early phase of adipogenesis. At this stage, only the ectopic expression of C/EBP- $\beta$  provides a surrogate for the requirement of adipogenic differentiation MIX by NIH-3T3 cells for differentiation (Wu et al. 1996). It is possible that further work in this area will generate novel opportunities to overcome the restricted subcutaneous adipogenesis which is predictive of type 2 diabetes.

Studies by Bowers and co-workers (Bowers et al. 2006) have previously demonstrated stem cell commitment to the adipocyte lineage by 5-Azacytidine inhibition of DNA methylation. These same investigators also provided evidence supporting the role of BMP4 signaling in the 5-Azacytidine-induced adipocyte lineage determination (Huang et al. 2009). Additional studies also revealed that increased expression and secretion of BMP4, a key molecule in the adipogenic microenvironment since it is also secreted by mature adipose cells (Gustafson et al. 2015), correlate with MSCs capacity to undergo adipogenic differentiation (Huang et al. 2009, Tang et al. 2004). Importantly, BMP4 was shown to enable nuclear entry of ZFP423 by dissociating the cytoplasmic WISP2-ZFP423 protein complex which retains ZFP423 in the cytosol (Hammarstedt et al. 2013), thereby activating *Ppar $\gamma$*  transcription. Silencing *Zfp423*

completely prevents the induction of *Ppar $\gamma$*  and other adipogenic marker genes in BMP4-treated cells, showing that ZFP423 is crucial for *Ppar $\gamma$*  activation as well as for the ability of BMP4 to induce *Ppar $\gamma$*  transcription (Hammarstedt et al. 2013).

In the present work, we demonstrate, for the first time, that BMP4 also causes demethylation of the *Zfp423* promoter, which is sufficient to commit otherwise non- adipogenic cells to the adipogenic lineage. Thus, convergence of the BMP4 signalling on *Zfp423* enables its action on preadipocyte determination through multiple mechanisms, including epigenetic modifications at key genes and nuclear import of ZFP423.

Interestingly BMP2, a BMP4 homolog, only slightly reduces *Zfp423* expression in NIH-3T3 cells (data not shown), likely because, as previously reported (Kamiya et al. 2011) the BMP2 target and *Zfp423* inhibitor ZFP521 is expressed in these cells. Addison et al. have indeed reported that BMP2-induced commitment of MSC to the adipose lineage is likely suppressed by ZFP521 through direct inhibition of *Zfp423*, providing a potential explanation for why BMP2 responses are predominantly osteogenic (Addison et al. 2014).

Detailed analysis of BMP4 action on *Zfp423* transcription revealed that BMP4-induced demethylation selectively involved the CpG dinucleotide at position -1016 from the *Zfp423* TSS. Interestingly methylation at this same site was invariably inhibited following 5-Azacytidine treatment of NIH-3T3 cells. These novel findings suggest a functional relevance of the -1016 dinucleotide. In fact, subsequent mutagenesis experiments demonstrated that, while not affecting the *in-vitro* function of the demethylated *Zfp423* promoter, the introduction of a point mutation at the -1016 CpG position prevented the methylation-dependent silencing of *Zfp423* transcription. Accordingly, we suggest that the regulatory effect of methylation at the *Zfp423* promoter is not only dependent upon the quantitative dimension of the methylation events but also on the specific promoter region which is affected.

Restricted adipogenesis in human SAT is determined by impaired adipocyte precursor cell commitment and results in hypertrophy of adipocytes in the SAT (Gustafson et al. 2013, Isakson et al. 2005, Arner et al. 2010) . Importantly, our recent studies have shown that markers of a restricted subcutaneous adipogenesis with inappropriate adipose cell hypertrophy are associated with a family history for type 2 diabetes (Arner et al. 2010, Smith et al. 2016) and also present in non-obese individuals with type 2 diabetes (Acosta et al. 2016). The relevance of our mechanistic findings in the NIH-3T3/3T3-L1 cell model to human adipose tissue dysfunction is underlined by our results in human adipocyte precursors revealing that their expression of the *Zfp423* human ortholog *ZNF423* (Harder et al. 2013) negatively correlates with the cell size of mature adipocytes. Hence, in the same individuals, low *ZNF423* expression in SVF preadipocytes is a marker of impaired adipogenesis leading to inappropriate



hypertrophy of mature subcutaneous adipocytes and causally contributing to it by interfering with precursor cell adipogenic commitment and differentiation.

Taken together, our present results suggest that the restricted subcutaneous adipogenesis associated with insulin resistance and a family history of type 2 diabetes may be due to dysfunctional epigenetic regulation rather than conventional DNA risk genes.

Secretion of BMP4 by mature adipose cells is positively correlated with adipose cells size and we have suggested that this is part of a positive feed-back in the tissue to enhance commitment and differentiation of new precursor cells to prevent inappropriate hypertrophy (Gustafson et al. 2015). We here provide a molecular basis for the effect of BMP4 to enhance adipogenesis although secretion of the BMP4 antagonists, in particular Gremlin 1 in man (Gustafson et al. 2015), is increased in hypertrophic obesity and prevents the expected positive effect of BMP4 on adipogenesis.

The overall structure of the regulatory regions of human *ZNF423* and mouse *Zfp423* is quite different (Harder et al. 2013). However, we observed massive hypermethylation at distinct CpG dinucleotides in the central island serving as promoter enhancer in human *ZNF423*. Hypermethylation of this same island has been previously shown to silence the gene in human leukaemia cells (Harder et al. 2013). The position of the regulatory CpG dinucleotides, which are targeted by methylation events in leukaemia and adipocyte precursor cells differ, likely reflecting tissue specificity (Ghosh et al. 2010). However, as demonstrated in the leukaemia cells, methylation at the preadipocyte *ZNF423* central enhancer island may also feature a repressive function as its presence closely correlated with the reduced *ZNF423* expression in the adipocyte precursor cells. We propose, therefore, that changes in the methylation profile at the regulatory region account for the reduced *ZNF423* expression observed in hypertrophic adipose tissue. Indeed, 5-Azacytidine treatment of preadipocytes isolated from individuals with adipose cell hypertrophy rescues both the hypomethylated and permissive state at specific CpG enhancer region dinucleotides and *ZNF423* expression.

Thus, based on our findings, methylation at the *ZNF423* regulatory region and its expression can be targeted both pharmacologically (i.e. 5-Azacytidine) and by changes in the microenvironment of the adipose tissue (i.e. changes in BMP4 abundance/signaling). Expansion of this work may generate attractive and novel opportunities to overcome the restricted subcutaneous adipogenesis and prevent inappropriate adipose tissue hypertrophy and its negative consequences on metabolism and risk of type 2 diabetes.

## 6. REFERENCES

Acosta JR, Douagi I, Andersson DP, Bäckdahl J, Rydén M, Arner P, Laurencikiene J. Increased fat cell size: a major phenotype of subcutaneous white adipose tissue in non-obese individuals with type 2 diabetes. *Diabetologia*. 2016 Mar;59(3):560-70.

Addison WN, Fu MM, Yang HX, Lin Z, Nagano K, Gori F, Baron R. Direct transcriptional repression of Zfp423 by Zfp521 mediates a bone morphogenic protein-dependent osteoblast versus adipocyte lineage commitment switch. *Mol Cell Biol*. 2014 Aug;34(16):3076-85.

Ahmadian M, Suh JM, Hah N, Liddle C, Atkins AR, Downes M, Evans RM. PPAR $\gamma$  signaling and metabolism: the good, the bad and the future. *Nat Med*. 2013 May;19(5):557-66.

Al-Goblan AS, Al-Alfi MA, Khan MZ. Mechanism linking diabetes mellitus and obesity. *Diabetes Metab Syndr Obes*. 2014 Dec 4;7:587-91.

Allison DB, Faith MS, Nathan JS. Risch's lambda values for human obesity. *Int J Obes Relat Metab Disord*. 1996 Nov;20(11):990-9.

American Diabetes Association. Approaches to Glycemic Treatment. *Diabetes Care* (Jan 2015); Volume 38, Supplement 1: S41–S48.

American Diabetes Association. Classification and Diagnosis of Diabetes. *Diabetes Care* 2015 Jan; 38 (Supplement 1): S8-S16.

American Diabetes Association. Diagnosis and Classification of Diabetes Mellitus. *Diabetes Care* (2010 Jan); 33(Suppl 1): S62–S69.

American Diabetes Association. Fast Facts-Data and Statistics about Diabetes. *DiabetesPro* (2014).

Appleton SL, Seaborn CJ, Visvanathan R, Hill CL, Gill TK, Taylor AW, Adams RJ; North West Adelaide Health Study Team. Diabetes and cardiovascular disease outcomes in the metabolically healthy obese phenotype: a cohort study. *Diabetes Care*. 2013 Aug;36(8):2388-94.

Arner P, Arner E, Hammarstedt A, Smith U. Genetic predisposition for Type 2 diabetes, but not for overweight/obesity, is associated with a restricted adipogenesis. *PLoS One*. 2011 Apr 12;6(4):e18284.

Aucott LS. Influences of weight loss on long-term diabetes outcomes. *Proc Nutr Soc.* 2008 Feb;67(1):54-9.

Bashan N, Dorfman K, Tarnowski T, Harman-Boehm I, Liberty IF, Blüher M, Ovadia S, Maymon-Zilberstein T, Potashnik R, Stumvoll M, Avinoach E, Rudich A. Mitogen-activated protein kinases, inhibitory-kappaB kinase, and insulin signaling in human omental versus subcutaneous adipose tissue in obesity. *Endocrinology.* 2007 Jun;148(6):2955-62.

Bell O, Tiwari VK, Thomä NH, Schübeler D. Determinants and dynamics of genome accessibility. *Nat Rev Genet.* 2011 Jul 12;12(8):554-64.

Blüher M. Adipose tissue dysfunction contributes to obesity related metabolic diseases. *Best Pract Res Clin Endocrinol Metab.* 2013 Apr;27(2):163-77.

Bouloumié A1, Lolmède K, Sengenès C, Galitzky J, Lafontan M. Angiogenesis in adipose tissue. *Ann Endocrinol (Paris).* 2002 Apr;63(2 Pt 1):91-5.

Bowers RR, Kim JW, Otto TC, Lane MD. Stable stem cell commitment to the adipocyte lineage by inhibition of DNA methylation: role of the BMP-4 gene. *Proc Natl Acad Sci U S A.* 2006 Aug 29;103(35):13022-7.

Britton KA, Fox CS. Ectopic fat depots and cardiovascular disease. *Circulation.* 2011 Dec 13;124(24):e837-41.

Brown RE, Kuk JL. Consequences of obesity and weight loss: a devil's advocate position. *Obes Rev.* 2015 Jan;16(1):77-87.

Cannon B, Nedergaard J. Brown adipose tissue: function and physiological significance. *Physiol Rev.* 2004 Jan;84(1):277-359.

Chaurasia B, Summers SA. Ceramides - Lipotoxic Inducers of Metabolic Disorders. *Trends Endocrinol Metab.* 2015 Oct;26(10):538-50.

Chen Z, Ishibashi S, Perrey S, Osuga Ji, Gotoda T, Kitamine T, Tamura Y, Okazaki H, Yahagi N, Iizuka Y, Shionoiri F, Ohashi K, Harada K, Shimano H, Nagai R, Yamada N. Troglitazone inhibits atherosclerosis in apolipoprotein E-knockout mice: pleiotropic effects on CD36 expression and HDL. *Arterioscler Thromb Vasc Biol.* 2001 Mar;21(3):372-7.

Choi SW, Claycombe KJ, Martinez JA, Friso S, Schalinske KL. Nutritional epigenomics: a portal to disease prevention. *Adv Nutr.* 2013 Sep 1;4(5):530-2.

Christodoulides C, Lagathu C, Sethi JK, Vidal-Puig A. Adipogenesis and WNT signalling. *Trends Endocrinol Metab.* 2009 Jan;20(1):16-24.

Chung WK, Leibel RL Considerations regarding the genetics of obesity. *Obesity* (Silver Spring). 2008 Dec;16 Suppl 3:S33-9.

Corvera S, Gealekman O. Adipose tissue angiogenesis: impact on obesity and type-2 diabetes. *Biochim Biophys Acta*. 2014 Mar;1842(3):463-72.

Dalle Grave R, Centis E, Marzocchi R, El Ghoch M, Marchesini G. Major factors for facilitating change in behavioral strategies to reduce obesity. *Psychol Res Behav Manag*. 2013 Oct 3;6:101-10.

Davis KE, D Neinast M, Sun K, M Skiles W, D Bills J, A Zehr J, Zeve D, D Hahner L, W Cox D, M Gent L, Xu Y, V Wang Z, A Khan S, Clegg DJ. The sexually dimorphic role of adipose and adipocyte estrogen receptors in modulating adipose tissue expansion, inflammation, and fibrosis. *Mol Metab*. 2013 Jun 4;2(3):227-42.

Deaton AM, Bird A. CpG islands and the regulation of transcription. *Genes Dev*. 2011 May 15;25(10):1010-22.

Deng Y, Scherer PE. Adipokines as novel biomarkers and regulators of the metabolic syndrome. *Ann N Y Acad Sci*. 2010 Nov;1212:E1-E19.

Denis GV, Obin MS. 'Metabolically healthy obesity': origins and implications. *Mol Aspects Med*. 2013 Feb;34(1):59-70.

El-Osta A, Brasacchio D, Yao D, Pocai A, Jones PL, Roeder RG, Cooper ME, Brownlee M. Transient high glucose causes persistent epigenetic changes and altered gene expression during subsequent normoglycemia. *J Exp Med*. 2008 Sep 29;205(10):2409-17.

Evans RM, Barish GD, Wang YX. PPARs and the complex journey to obesity. *Nat Med*. 2004 Apr;10(4):355-61.

Farmer SR. Regulation of PPARgamma activity during adipogenesis. *Int J Obes (Lond)*. 2005 Mar;29 Suppl 1:S13-6.

Fujiki K, Kano F, Shiota K, Murata M. Expression of the peroxisome proliferator activated receptor gamma gene is repressed by DNA methylation in visceral adipose tissue of mouse models of diabetes. *BMC Biol*. 2009 Jul 10;7:38.

Gealekman O, Guseva N, Hartigan C, Apotheker S, Gorgoglione M, Gurav K, Tran KV, Straubhaar J, Nicoloso S, Czech MP, Thompson M, Perugini RA, Corvera S. Depot-specific differences and insufficient subcutaneous adipose tissue angiogenesis in human obesity. *Circulation*. 2011 Jan 18;123(2):186-94.

Ghosh S, Yates AJ, Frühwald MC, Miecznikowski JC, Plass C, Smiraglia D. Tissue specific DNA methylation of CpG islands in normal human adult somatic tissues distinguishes neural from non-neural tissues. *Epigenetics*. 2010 Aug 16;5(6):527-38.

Greenberg AS, Obin MS. Obesity and the role of adipose tissue in inflammation and metabolism. *Am J Clin Nutr* (2006 Feb); 83(2):461S – 465S.

Guh DP, Zhang W, Bansback N, Amarsi Z, Birmingham CL, Anis AH. The incidence of co-morbidities related to obesity and overweight: a systematic review and meta-analysis. *BMC Public Health*. 2009 Mar 25;9:88.

Gupta RK, Arany Z, Seale P, Mepani RJ, Ye L, Conroe HM, Roby YA, Kulaga H, Reed RR, Spiegelman BM. Transcriptional control of preadipocyte determination by Zfp423. *Nature*. 2010 Mar 25;464(7288):619-23.

Gupta RK, Mepani RJ, Kleiner S, Lo JC, Khandekar MJ, Cohen P, Frontini A, Bhowmick DC, Ye L, Cinti S, Spiegelman BM. Zfp423 expression identifies committed preadipocytes and localizes to adipose endothelial and perivascular cells. *Cell Metab*. 2012 Feb 8;15(2):230-9.

Gustafson B, Hammarstedt A, Andersson CX, Smith U. Inflamed adipose tissue: a culprit underlying the metabolic syndrome and atherosclerosis. *Arterioscler Thromb Vasc Biol*. 2007 Nov;27(11):2276-83.

Gustafson B, Hammarstedt A, Hedjazifar S, Hoffmann JM, Svensson PA, Grimsby J, Rondinone C, Smith U. BMP4 and BMP Antagonists Regulate Human White and Beige Adipogenesis. *Diabetes*. 2015 May;64(5):1670-81.

Gustafson B, Hammarstedt A, Hedjazifar S, Smith U. Restricted adipogenesis in hypertrophic obesity: the role of Wisp2, WNT, and Bmp4. *Diabetes*. 2013 Sep;62(9):2997-3004.

Gustafson B, Hedjazifar S, Gogg S, Hammarstedt A, Smith U. Insulin resistance and impaired adipogenesis. *Trends Endocrinol Metab*. 2015 Apr;26(4):193-200.

Gustafson B, Smith U. The WNT inhibitor Dickkopf 1 and bone morphogenetic protein 4 rescue adipogenesis in hypertrophic obesity in humans. *Diabetes*. 2012 May;61(5):1217-24.

Gustafson B. Adipose tissue, inflammation and atherosclerosis. *J Atheroscler Thromb*. 2010 Apr 30;17(4):332-41.

Hammarstedt A, Hedjazifar S, Jenndahl L, Gogg S, Grünberg J, Gustafson B, Klimcakova E, Stich V, Langin D, Laakso M, Smith U. Wisp2 regulates preadipocyte commitment and Ppar $\gamma$  activation by Bmp4. *Proc Natl Acad Sci U S A*. 2013 Feb 12;110(7):2563-8.

Harder L, Eschenburg G, Zech A, Kriebitzsch N, Otto B, Streichert T, Behlich AS, Dierck K, Klingler B, Hansen A, Stanulla M, Zimmermann M, Kremmer E, Stocking C, Horstmann MA. Aberrant ZNF423 impedes B cell differentiation and is linked to adverse outcome of ETV6-RUNX1 negative B precursor acute lymphoblastic leukemia. *J Exp Med*. 2013 Oct 21;210(11):2289-304.

Harris MI, Flegal KM, Cowie CC, Eberhardt MS, Goldstein DE, Little RR, Wiedmeyer HM, Byrd-Holt DD. Prevalence of diabetes, impaired fasting glucose, and impaired glucose tolerance in U.S. adults. The Third National Health and Nutrition Examination Survey, 1988-1994. *Diabetes Care*. 1998 Apr;21(4):518-24.

Harrison. *Principi di Medicina Interna. Il Manuale* 17/ed March 2009.

Hepler C, Gupta RK. The expanding problem of adipose depot remodeling and postnatal adipocyte progenitor recruitment. *Mol Cell Endocrinol*. 2017 Apr 15;445:95-108.

Herrera BM, Keildson S, Lindgren CM. Genetics and epigenetics of obesity. *Maturitas*. 2011 May;69(1):41-9.

Hirsch J, Han PW. Cellularity of rat adipose tissue: effects of growth, starvation, and obesity. *J Lipid Res*. 1969 Jan;10(1):77-82.

Huang H, Song TJ, Li X, Hu L, He Q, Liu M, Lane MD, Tang QQ. BMP signaling pathway is required for commitment of C3H10T1/2 pluripotent stem cells to the adipocyte lineage. *Proc Natl Acad Sci U S A*. 2009 Aug 4;106(31):12670-5.

International Diabetes Federation Atlas (IDF ATLAS). Sixth edition (2013).

Isakson P, Hammarstedt A, Gustafson B, Smith U. Impaired preadipocyte differentiation in human abdominal obesity: role of Wnt, tumor necrosis factor- $\alpha$ , and inflammation. *Diabetes*. 2009 Jul;58(7):1550-7.

Kamiya D, Banno S, Sasai N, Ohgushi M, Inomata H, Watanabe K, Kawada M, Yakura R, Kiyonari H, Nakao K, Jakt LM, Nishikawa S, Sasai Y. Intrinsic transition of embryonic stem-cell differentiation into neural progenitors. *Nature*. 2011 Feb 24;470(7335):503-9.

Karastergiou K, Smith SR, Greenberg AS, Fried SK. Sex differences in human adipose tissues - the biology of pear shape. *Biol Sex Differ*. 2012 May 31;3(1):13.

Karpe F, Pinnick KE. Biology of upper-body and lower-body adipose tissue--link to whole-body phenotypes. *Nat Rev Endocrinol*. 2015 Feb;11(2):90-100.

Kelly T, Yang W, Chen C-S, Reynolds K, He J. Global burden of obesity in 2005 and projections to 2030. *Int J Obes*. 2008 Sep;32(9):1431-7

Klingenberg M. Uncoupling protein-a useful energy dissipator. *J Bioenerg Biomembr*. 1999 Oct;31(5):419-30.

Klose RJ, Bird AP. Genomic DNA methylation: the mark and its mediators. *Trends Biochem Sci*. 2006 Feb;31(2):89-97.

Klötting N, Blüher M. Adipocyte dysfunction, inflammation and metabolic syndrome. *Rev Endocr Metab Disord*. 2014 Dec;15(4):277-87.

Klötting N, Fasshauer M, Dietrich A, Kovacs P, Schön MR, Kern M, Stumvoll M, Blüher M. Insulin-sensitive obesity. *Am J Physiol Endocrinol Metab*. 2010 Sep;299(3):E506-15.

Kopelman PG. Obesity as a medical problem. *Nature*. 2000 Apr 6;404(6778):635-43.

Laakso M, Zilinskaite J, Hansen T, Boesgaard TW, Vanttinen M, Stancáková A, Jansson PA, Pellmé F, Holst JJ, Kuulasmaa T, Hribal ML, Sesti G, Stefan N, Fritsche A, Häring H, Pedersen O, Smith U; EUGENE2 Consortium. Insulin sensitivity, insulin release and glucagon-like peptide-1 levels in persons with impaired fasting glucose and/or impaired glucose tolerance in the EUGENE2 study. *Diabetologia*. 2008 Mar;51(3):502-11.

Lee MJ, Wu Y, Fried SK. Adipose tissue heterogeneity: implication of depot differences in adipose tissue for obesity complications. *Mol Aspects Med*. 2013 Feb;34(1):1-11.

Lee YH, Thacker RI, Hall BE, Kong R, Granneman JG. Exploring the activated adipogenic niche: interactions of macrophages and adipocyte progenitors. *Cell Cycle*. 2014;13(2):184-90.

Logan CY, Nusse R. The Wnt signaling pathway in development and disease. *Annu Rev Cell Dev Biol*. 2004;20:781-810.

Lönn M, Mehlig K, Bengtsson C, Lissner L. Adipocyte size predicts incidence of type 2 diabetes in women. *FASEB J*. 2010 Jan;24(1):326-31.

Louet JF, O'Malley BW. Coregulators in adipogenesis: what could we learn from the SRC (p160) coactivator family? *Cell Cycle*. 2007 Oct 15;6(20):2448-52.

Macotela Y, Emanuelli B, Mori MA, Gesta S, Schulz TJ, Tseng YH, Kahn CR. Intrinsic differences in adipocyte precursor cells from different white fat depots. *Diabetes*. 2012 Jul;61(7):1691-9.

Martínez JA, Milagro FI, Claycombe KJ, Schalinske KL. Epigenetics in adipose tissue, obesity, weight loss, and diabetes. *Adv Nutr*. 2014 Jan 1;5(1):71-81.

Musri MM, Gomis R, Párrizas M. A chromatin perspective of adipogenesis. *Organogenesis*. 2010 Jan-Mar;6(1):15-23.

Neeland IJ, Turer AT, Ayers CR, et al. Dysfunctional adiposity and the risk of prediabetes and type 2 diabetes in obese adults. *JAMA*. 2012 Sep 19;308(11):1150-9.

Ni Mhurchu C, Parag V, Nakamura M, Patel A, Rodgers A, Lam TH, Asia Pacific Cohort Studies Collaboration. Body mass index and risk of diabetes mellitus in the Asia-Pacific region. *Asia Pac J Clin Nutr*. 2006;15(2):127-33.

Organization for Economic Cooperation Development (OECD) Health Statistics; Eurostat Statistics Database; WHO Global Health Expenditure Database (2014).

Organization for Economic Cooperation Development (OECD). Obesity and the Economics of Prevention: Fit not Fat Key Facts – Italy, Update 2014 [Online]

Palmer BF, Clegg DJ. The sexual dimorphism of obesity. *Mol Cell Endocrinol*. 2015 Feb 15;402:113-9.

Pardo M, Roca-Rivada A, Seoane LM, Casanueva FF. Obesidomics: contribution of adipose tissue secretome analysis to obesity research. *Endocrine*. 2012 Jun;41(3):374-83.

Perry RJ, Samuel VT, Petersen KF, Shulman GI. The role of hepatic lipids in hepatic insulin resistance and type 2 diabetes. *Nature*. 2014 Jun 5;510(7503):84-91.

Pinnick KE, Karpe F. DNA methylation of genes in adipose tissue. *Proc Nutr Soc*. 2011 Feb;70(1):57-63.

Rajakumari S, Wu J, Ishibashi J, Lim HW, Giang AH, Won KJ, Reed RR, Seale P. EBF2 determines and maintains brown adipocyte identity. *Cell Metab*. 2013 Apr 2;17(4):562-74.

Reaven GM. Pathophysiology of insulin resistance in human disease. *Physiol Rev*. 1995 Jul;75(3):473-86.

Resnick HE, Valsania P, Halter JB, Lin X. Relation of weight gain and weight loss on subsequent diabetes risk in overweight adults. *J Epidemiol Community Health*. 2000 Aug;54(8):596-602.

Ricote M, Li AC, Willson TM, Kelly CJ, Glass CK. The peroxisome proliferator-activated receptor-gamma is a negative regulator of macrophage activation. *Nature*. 1998 Jan 1;391(6662):79-82.



Ricoult SJ, Manning BD. The multifaceted role of mTORC1 in the control of lipid metabolism. *EMBO Rep*. 2013 Mar 1;14(3):242-51.

Romao JM, Jin W, Dodson MV, Hausman GJ, Moore SS, Guan LL. MicroRNA regulation in mammalian adipogenesis. *Exp Biol Med (Maywood)*. 2011 Sep;236(9):997-1004.

Ronti T, Lupattelli G, Mannarino E. The endocrine function of adipose tissue: an update. *Clin Endocrinol (Oxf)*. 2006 Apr;64(4):355-65.

Rosen ED, MacDougald OA. Adipocyte differentiation from the inside out. *Nat Rev Mol Cell Biol*. 2006 Dec;7(12):885-96.

Rosen ED, Spiegelman BM. Adipocytes as regulators of energy balance and glucose homeostasis. *Nature*. 2006 Dec 14;444(7121):847-53.

Rosen ED, Spiegelman BM. What we talk about when we talk about fat. *Cell*. 2014 Jan 16;156(1-2):20-44.

Rudich A, Kanety H, Bashan N. Adipose stress-sensing kinases: linking obesity to malfunction. *Trends Endocrinol Metab*. 2007 Oct;18(8):291-9.

Rytka JM, Wueest S, Schoenle EJ, Konrad D. The portal theory supported by venous drainage-selective fat transplantation. *Diabetes*. 2011 Jan;60(1):56-63.

Sattar N, Gill JM. Type 2 diabetes as a disease of ectopic fat?. *BMC Med*. 2014 Aug 26;12:123.

Sell H, Habich C, Eckel J. Adaptive immunity in obesity and insulin resistance. *Nat Rev Endocrinol*. 2012 Dec;8(12):709-16.

Shao M, Ishibashi J, Kusminski CM, Wang QA, Hepler C, Vishvanath L, MacPherson KA, Spurgin SB, Sun K, Holland WL, Seale P, Gupta RK. Zfp423 Maintains White Adipocyte Identity through Suppression of the Beige Cell Thermogenic Gene Program. *Cell Metab*. 2016 Jun 14;23(6):1167-1184.

Smith U, Hammarstedt A. Antagonistic effects of thiazolidinediones and cytokines in lipotoxicity. *Biochim Biophys Acta*. 2010 Mar;1801(3):377-80.

Smith U, Kahn BB. Adipose tissue regulates insulin sensitivity: role of adipogenesis, de novo lipogenesis and novel lipids. *J Intern Med*. 2016 Nov;280(5):465-475.

Spalding KL, Arner E, Westermarck PO, Bernard S, Buchholz BA, Bergmann O, Blomqvist L, Hoffstedt J, Näslund E, Britton T, Concha H, Hassan M, Rydén M, Frisén J, Arner P. Dynamics of fat cell turnover in humans. *Nature*. 2008 Jun 5;453(7196):783-7.

Speakman JR. Obesity: the integrated roles of environment and genetics. *J Nutr.* 2004 Aug;134(8 Suppl):2090S-2105S.

Sun K, Kusminski CM, Scherer PE. Adipose tissue remodeling and obesity. *J Clin Invest.* 2011 Jun;121(6):2094-101.

Tabish SA. Is Diabetes Becoming the Biggest Epidemic of the Twenty-first Century? *Int J Health Sci (Qassim).* 2007 Jul;1(2):V-VIII.

Talchai C, Xuan S, Lin HV, Sussel L, Accili D. Pancreatic b cell dedifferentiation as a mechanism of diabetic b cell failure. *Cell.* 2012 Sep 14;150(6):1223-34.

Talman AH, Psaltis PJ, Cameron JD, Meredith IT, Seneviratne SK, Wong DT. Epicardial adipose tissue: far more than a fat depot. *Cardiovasc Diagn Ther.* 2014 Dec;4(6):416-29.

Tang QQ, Lane MD. Adipogenesis: from stem cell to adipocyte. *Annu Rev Biochem.* 2012;81:715-36.

Tang QQ, Otto TC, Lane MD. Commitment of C3H10T1/2 pluripotent stem cells to the adipocyte lineage. *Proc Natl Acad Sci U S A.* 2004 Jun 29;101(26):9607-11.

Tannock LR, Little PJ, Tsoi C, Barrett PH, Wight TN, Chait A. Thiazolidinediones reduce the LDL binding affinity of non-human primate vascular cell proteoglycans. *Diabetologia.* 2004 May;47(5):837-43.

Tchoukalova YD, Votruba SB, Tchkonja T, Giorgadze N, Kirkland JL, Jensen MD. Regional differences in cellular mechanisms of adipose tissue gain with overfeeding. *Proc Natl Acad Sci U S A.* 2010 Oct 19;107(42):18226-31.

Tontonoz P, Hu E, Spiegelman BM. Stimulation of adipogenesis in fibroblasts by PPAR gamma 2, a lipid-activated transcription factor. *Cell.* 1994 Dec 30;79(7):1147-56.

Tran TT, Yamamoto Y, Gesta S, Kahn CR. Beneficial effects of subcutaneous fat transplantation on metabolism. *Cell Metab.* 2008 May;7(5):410-20.

Van Harmelen V, Röhrig K, Hauner H. Comparison of proliferation and differentiation capacity of human adipocyte precursor cells from the omental and subcutaneous adipose tissue depot of obese subjects. *Metabolism.* 2004 May;53(5):632-7.

Weisberg SP, McCann D, Desai M, Rosenbaum M, Leibel RL, Ferrante AW Jr. Obesity is associated with macrophage accumulation in adipose tissue. *J Clin Invest.* 2003 Dec;112(12):1796-808.

World Health Organization. Global status report on non-communicable diseases. WHO Library Cataloguing-in-Publication Data (2010).

World Health Organization. Obesity and Overweight. Facts. Geneva: World Health Organization (2014).

Wu J, Boström P, Sparks LM, Ye L, Choi JH, Giang AH, Khandekar M, Virtanen KA, Nuutila P, Schaart G, Huang K, Tu H, van Marken Lichtenbelt WD, Hoeks J, Enerbäck S, Schrauwen P, Spiegelman BM. Beige adipocytes are a distinct type of thermogenic fat cell in mouse and human. *Cell*. 2012 Jul 20;150(2):366-76.

Wu Z, Bucher NL, Farmer SR. Induction of peroxisome proliferator-activated receptor gamma during the conversion of 3T3 fibroblasts into adipocytes is mediated by C/EBPbeta, C/EBPdelta, and glucocorticoids. *Mol Cell Biol*. 1996 Aug;16(8):4128-36.

Yaturu S. Obesity and type 2 diabetes. *Journal of Diabetes Mellitus* 2011;Vol.1, No.4, 79-95.